



PAN AFRICAN UNIVERSITY
INSTITUTE FOR BASIC SCIENCES,
TECHNOLOGY AND INNOVATION



MASTER THESIS

**STRUCTURAL CHARACTERISATION AND PERFORMANCE
EVALUATION OF THE FAILED MANAFWA HISTORIC
BRIDGE IN UGANDA**

MASTER OF SCIENCE IN CIVIL ENGINEERING
(STRUCTURAL OPTION)

IGA DAN - CE300-0006/2015

Thesis Submitted to the Pan African University – Institute of Science, Technology and Innovation in Partial Fulfilment of the Requirement for Award of the Degree of Master of Science in Civil Engineering.

MAY 2018

DECLARATION

I, **IGA DAN**, the undersigned do solemnly declare to the best of my knowledge and effort that was initiated by me and unless otherwise referenced, the contents have never been submitted to any university for any academic achievements.

Signature Date

Iga Dan

This Research Thesis has been submitted with our approval as University supervisors:

Signature..... Date.....

Dr. (Eng.) Timothy Nyomboi

Department of Civil and Structural Engineering, Moi University, Kenya

Signature Date

Prof. (Eng.) Richard Ocharo Onchiri

Department of Building and Civil Engineering, Technical University of Mombasa

Signature Date

Dr. Moses Matovu

College of Engineering, Design, Art and Technology, Makerere University

DEDICATION

To

My dear mummy,

Miss Naluyima Miriam N.

She single handedly sacrificed and struggled to bring me thus far; without her, am not. I LOVE U

ACKNOWLEDGEMENTS

There are very many people I would like to thank, especially the following;

- The Almighty God for having given me the greatest gift of Life to go through the Research period successfully and for sparing my life to ensure that I finish my studies.
- To the Pan African University – PAU that is committed to the provision of the opportunity for advanced graduate training and postgraduate research to high-performing African students through the PAU scholarship grants, without this scholarship I wouldn't have gotten the privilege of pursuing this MSc.
- To my Research Project supervisors, Dr. T. Nyomboi, Prof. Richard Ocharo and Dr. Matovu Moses, am very indebted for the technical advice, support, encouragement, counsel and guidance.
- To my classmates; Almaleh Abubaker, Leolin Deffo Deffo Rostand, Nathalie Mao, Idowu Temitope Ezekiel and Ismael Ouedrago; you guys are amazing and I am very fortunate to have spent my time with great men and lady who will greatly impact the African Continent with advances in the Civil Engineering fraternity.
- To the entire PAU fraternity, from the Director, all my lecturers, the Structural laboratory of JKUAT laboratory technicians Mr. Obadiah and Mr. Karugu, the technicians from the Structural Laboratory of Makerere University Mr. Ntume William and Mr. Kanamwanjje and my classmates. Thanks for your support.
- My great mother Miss. Naluyima Miriam and my whole family for the great support and encouragement they offered me. And in addition, my work supervisors Eng. Christopher Manyindo and Eng. Phillip Kitimba Patrick for your support and counsel. Your contributions cannot go unnoticed.

ABSTRACT

The Manafwa Bridge is located in Busiu Sub County located in Mbale District. A part of the bridge located on the Mbale – Tororo Highway caved in leaving a very large hole in the middle of the bridge resulting into paralysis of traffic along the road that links the Northern part of Uganda and Southern Sudan to the Central part of Uganda. Consequently, traffic along the road was disturbed hence impacting on the economy as the route is a key linkage to Southern Sudan and to Kenya.

Uganda has many similar historic bridges that were constructed in the middle of the 20th Century and yet the demand for new bridges in many other areas is very high. In order to meet future transportation demands, the study was conducted to find means of improving the existing historic bridges. One way to achieve this is by predicting the failure mechanism of the Manafwa bridge and others that collapsed in the recent past and to investigate means of increasing the load carrying capacity of existing bridges to allow heavier traffic to pass.

The study involved bridge inspections and condition assessment surveys of the bridge and carrying out of field testing (both destructive and non-destructive tests) on the two-span Manafwa River Bridge along Mbale - Tororo Road to assess the extent of damage caused by traffic to the bridge superstructure. The superstructure slab developed a hole between two longitudinal steel beams located adjacent to the carriageway centre line on the Mbale bound lane on the Tororo span. There was noticeable cracking of the deck surfacing at a corresponding location on the Mbale span. Traffic counts were also carried out to determine the traffic loading on the bridge and axle load information generated.

This study included structural assessment with experimental model analysis of the punching shear capacity of the bridge deck slab model. A numerical simulation of the entire bridge superstructure was carried out and of the failed deck slab area using ANSYS 16.0. The main findings of the study show that the deck slab failed because of deterioration of the concrete with in-situ results showing compressive strength of 9MPa in contrast to the design strength of 30MPa and the lack of hogging reinforcement. Punching shear due to the wheel loads exerted on the road led to the eventual development of the hole in the deck slab.

The study recommends that a 200mm structural topping slab can be applied to the existing slab of minimum class 30/19 structurally bonded to the existing slab instead of demolishing the bridge. The study also recommends that this approach should be taken up for all other Historic Bridges to improve their performance and service life.

Key Words: Bridge Deck Slab, Structural Assessment and Evaluation, Punching Shear Behaviour of Structures, Numerical Modelling.

TABLE OF CONTENTS:

DECLARATION	I
DEDICATION	II
ACKNOWLEDGEMENTS	III
ABSTRACT.....	IV
TABLE OF CONTENTS:.....	V
LIST OF FIGURES	VIII
LIST OF PLATES	IX
LIST OF TABLES.....	X
CHAPTER 1. INTRODUCTION.....	1
1.1 BACKGROUND TO THE STUDY	1
1.2 STATEMENT OF THE RESEARCH PROBLEM.....	1
1.3 RESEARCH OBJECTIVES	3
1.3.1 <i>Main Objectives</i>	3
1.3.2 <i>Specific Objectives</i>	3
1.4 SCOPE OF WORK.....	3
1.5 JUSTIFICATION	3
CHAPTER 2. LITERATURE REVIEW.....	5
2.1 INTRODUCTION – BRIDGE TYPES AND CHARACTERISTICS	5
2.1.1 <i>Simply supported Beam/Girder bridges</i>	5
2.1.2 <i>Arch bridge</i>	6
2.1.3 <i>The suspension bridge</i>	6
2.1.4 <i>Steel truss bridges</i>	7
2.1.5 <i>Types of bridge decks</i>	7
2.2 BRIDGE STRUCTURAL ANALYSIS	8
2.2.1 <i>Common structural and material defects (concrete) in bridge structures</i>	9
2.2.2 <i>Non Destructive Testing of Bridge</i>	9
2.2.3 <i>Schmidt Rebound Hammer Test</i>	11
2.2.4 <i>Core Test</i>	11
2.3 STRUCTURAL RESPONSE OF REINFORCED CONCRETE SLABS	12
2.3.1 <i>Failure Modes</i>	12
2.3.2 <i>Punching shear failure mechanism</i>	13
2.3.3 <i>Review of research carried out and experimental model for reinforced concrete slabs</i>	14
2.3.4 <i>FIELD TEST OF A BRIDGE DECK SLAB</i>	15
2.4 FINITE ELEMENT METHOD	17
2.4.1 <i>The finite element method and element formulations</i>	17
2.4.2 <i>Finite element modelling and analysis of reinforced-concrete bridge decks</i>	17

2.4.3	<i>Finite element modelling and analysis using ABACUS</i>	18
2.4.4	<i>Numerical Modelling and Validation of Composite Bridge Decking</i>	18
2.4.5	<i>Finite element analysis of a composite bridge deck</i>	21
2.5	RESEARCH GAP – MANAFWA BRIDGE COMPARISONS TO TESTED BRIDGES	22
CHAPTER 3. RESEARCH METHODOLOGY		24
3.1	INTRODUCTION	24
3.2	STRUCTURAL CHARACTERIZATION OF THE FAILED HISTORIC BRIDGE.....	24
3.2.1	<i>Desk study and site reconnaissance of the Manafwa Bridge</i>	24
3.2.2	<i>Condition Assessment Survey</i>	25
3.2.3	<i>Non – Destructive Testing using Rebound Hammer</i>	25
3.2.4	<i>Destructive Testing using Coring</i>	27
3.2.5	<i>Structural Steel Reinforcement –Tensile Strength Tests</i>	28
3.3	NUMERICAL ANALYSIS OF THE HISTORIC BRIDGE.....	28
3.3.1	<i>Introduction</i>	28
3.3.2	<i>FEM Input Data</i>	29
3.3.3	<i>Bridge Loads determination - Traffic inventory and assessment</i>	29
3.3.4	<i>ANSYS Modelling</i>	29
3.4	EXPERIMENTAL MODELLING OF THE BRIDGE DECK SLAB	31
3.4.1	<i>Definition of the scope of the problem/experimental testing</i>	31
3.4.2	<i>Specifying of similitude requirements for geometry, materials and loading</i>	31
3.4.3	<i>Sizing of the physical model</i>	31
3.4.4	<i>Selection of Model Materials</i>	32
3.4.5	<i>Fabrication phase of the Deck Slabs</i>	32
3.4.6	<i>Instrumentation and recording equipment for displacements and forces</i>	33
3.4.7	<i>Loading Systems and Conditions</i>	33
CHAPTER 4. RESULTS, DISCUSSION AND ANALYSIS		35
4.1	STRUCTURAL CHARACTERIZATION OF THE FAILED HISTORIC BRIDGE.....	35
4.1.1	<i>Conditional Assessment Survey of the Bridge</i>	35
4.1.2	<i>Bridge Superstructure Geometry</i>	36
4.1.3	<i>Steel I-Beam Section</i>	37
4.1.4	<i>Visual Inspection photography</i>	38
4.1.5	<i>Schmidt’s Rebound Hammer Test Results</i>	39
4.1.6	<i>Destructive Test Results - Core Test</i>	40
4.1.7	<i>Structural Steel tensile strength Tests</i>	41
4.2	STRUCTURAL EVALUATION AND ASSESSMENT.....	43
4.2.1	<i>Superstructure Slab Shear Capacity Under Concentrated Loads</i>	43
4.2.2	<i>Superstructure Slab Moment Capacity</i>	46
4.3	EXPERIMENTAL MODEL - LABORATORY RESULTS OBTAINED	48
4.3.1	<i>Concrete Mix Design for the 30MPa and 13MPa Deck Slabs</i>	48
4.3.2	<i>28MPa Deck Slab (depicting the Design bridge condition):</i>	49
4.3.3	<i>13MPa Deck Slab (depicting the Design bridge condition):</i>	51

4.4	NUMERICAL ANALYSIS OF THE HISTORIC BRIDGE.....	53
4.4.1	<i>Total Deformation of the entire bridge (Global Solution).....</i>	<i>54</i>
4.4.2	<i>Total Deformation of the Failed Bridge element (Particular Solution).....</i>	<i>55</i>
4.5	COMPARISON OF EXPERIMENTAL AND NUMERICAL ANALYSIS RESULTS ...	56
4.5.1	<i>The Numerical analysis of the bridge failure model.....</i>	<i>56</i>
4.5.2	<i>Structural Failure Mechanism using the Experimental Model</i>	<i>57</i>
CHAPTER 5. CONCLUSION AND RECOMMENDATION		59
5.1	CONCLUSIONS	59
5.2	RECOMMENDATIONS.....	59
5.2.1	<i>Recommendations of the Research</i>	<i>59</i>
5.2.2	<i>Recommended Areas for Further Research.....</i>	<i>60</i>
REFERENCES.....		61
APPENDIX.....		66
APPENDIX A. STRUCTURAL CHARACTERISATION TEST RESULTS FROM THE		
REBOUND HAMMER		
		66
APPENDIX B. DESTRUCTIVE TEST RESULTS FROM THE CORES TAKEN.....		
		68
APPENDIX C. STRUCTURAL STEEL LABORATORY TEST RESULTS.....		
		69
APPENDIX E. NUMERICAL ANALYSIS DATA		
		71
APPENDIX F. NUMERICAL ANALYSIS RESULTS DURING EVALUATION.....		
		72
APPENDIX G. EXPERIMENTAL TEST RESULTS.....		
		76
APPENDIX H. STANDARD VEHICLE CLASSIFICATION CHART.....		
		79
APPENDIX I. FORM FOR MANUAL CLASSIFIED TRAFFIC COUNTS.....		
		80
APPENDIX J. TRAFFIC DATA COLLECTED AND ANALYSED		
		80
APPENDIX K. EQUIPMENT LIST FOR TRAFFIC COUNT AND/OR AXLE LOAD		
SURVEY		
		82
APPENDIX L. CONCRETE MIX DESIGN – SAMPLE FORM USED AND MATERIAL		
RESULTS		
		83
APPENDIX M. BRIDGE INSPECTION REPORT – FILLED CONDITION ASSESSMENT		
SURVEY FORM		
		85

LIST OF FIGURES

<i>Figure 2-1 Simply supported I-girder bridge structure.....</i>	<i>5</i>
<i>Figure 2-2 The Old Trails Arch Bridge.....</i>	<i>6</i>
<i>Figure 2-3 Nile River suspension bridge being constructed in Uganda</i>	<i>6</i>
<i>Figure 2-4 Steel Truss bridge layout</i>	<i>7</i>
<i>Figure 2-5 Solid Slab.....</i>	<i>7</i>
<i>Figure 2-6 Voided Slab.....</i>	<i>8</i>
<i>Figure 2-7 Beam and Slab.....</i>	<i>8</i>
<i>Figure 2-8 Typical composite deck.....</i>	<i>8</i>
<i>Figure 2-10 Punching shear failure section in concrete deck due to concentrated load.....</i>	<i>13</i>
<i>Figure 2-11 Punching shear failure on the underside of the bridge deck due to concentrated load</i>	<i>13</i>
<i>Figure 2-12 Example of finite element structural analysis model of a double beam bridge.....</i>	<i>17</i>
<i>Figure 2-2 7600 tri-axle dump trucks used for live-load test.</i>	<i>20</i>
<i>Figure 2-3 Service load deflection.....</i>	<i>20</i>
<i>Figure 2-4 Tsai-Hill Index (R) ($\sqrt{I_{TH}}$) (LRFD).....</i>	<i>21</i>
<i>Figure 2-13 Geometry of the tested bridge (Shu, 2014).</i>	<i>23</i>
<i>Figure 2-14 Failed bridge deck slab after shear failure</i>	<i>23</i>
<i>Figure 3-1 A detailed overview of the research process</i>	<i>24</i>
<i>Figure 3-2 Conversion curve for the average compressive strength measured on cylinders.</i>	<i>26</i>
<i>Figure 3-3 Full bridge model as applied in the ANSYS program (Isometric 3-D view).....</i>	<i>30</i>
<i>Figure 3-4 Failed Deck slab Model.....</i>	<i>30</i>
<i>Figure 3-5 Processing of the Mathematical ANSYS solution ongoing.....</i>	<i>31</i>
<i>Figure 4-1 Manafwa River Bridge superstructure cross section</i>	<i>36</i>
<i>Figure 4-2 Steel beam cross section.....</i>	<i>37</i>
<i>Figure 4-3 In-Situ Concrete Strength Test Results From The Schmidt Rebound Hammer.....</i>	<i>39</i>
<i>Figure 4-4 Summary of the core compressive strength results of the deck slab</i>	<i>40</i>
<i>Figure 4-5 Field Crushing compressive strength of cylindrical cores obtained from the deck slab of the Manafwa Bridge</i>	<i>41</i>
<i>Figure 4-6 Tensile strength of the reinforcement bars</i>	<i>42</i>
<i>Figure 4-7 Chemical Analysis of Reinforcement Bars Tested in Accordance with BS 4449:2005</i>	<i>43</i>
<i>Figure 4-8 Shear Perimeter.....</i>	<i>44</i>
<i>Figure 4-9 Sieve analysis result of the sand.....</i>	<i>49</i>
<i>Figure 4-10 Sieve analysis result of the gravel</i>	<i>49</i>
<i>Figure 4-11 Graph for the Experimental mid-span deflection of the 28-day Deck Slab.....</i>	<i>50</i>
<i>Figure 4-12 Graph for the Experimental mid-span deflection of the 13MPa Deck Slab.....</i>	<i>53</i>
<i>Figure 4-13 Total Deformation of the superstructure deck slab system (Top view).....</i>	<i>54</i>
<i>Figure 4-14 Total Deformation shown using contour lines of the superstructure deck slab system</i>	<i>54</i>
<i>Figure 4-153 Von Misses Failure Criterion showing maximum stresses concentration</i>	<i>56</i>

LIST OF PLATES

<i>Plate 1-1 Collapse of the Mitooma Bridge and the Aswa Bridge respectively.....</i>	<i>2</i>
<i>Plate 1-2 Failure of the Manafwa Historic bridge.....</i>	<i>2</i>
<i>Plate 2-1 Traffic load tests to determine load capacity of composite decking.....</i>	<i>19</i>
<i>Plate 3-1 Schmidt Rebound Hammer used for the in-situ testing of the compressive strength.....</i>	<i>26</i>
<i>Plate 3-2 Core Testing being done on the deck's slab.....</i>	<i>28</i>
<i>Plate 3-3 Project Schematic indicating completion of the analysis.....</i>	<i>30</i>
<i>Plate 3-4 Experimental model scaled down using a geometric scale of 2.....</i>	<i>32</i>
<i>Plate 3-5 Fabrication process of the Deck Slab model in the laboratory.....</i>	<i>33</i>
<i>Plate 3-6 Transducer being configured prior to testing and Loading using a Load cell.....</i>	<i>34</i>
<i>Plate 3-7 Strain gauges connected to the transducer and the LVDT connected to the Loading Cell to measure deflection at the centre of the slab.....</i>	<i>34</i>
<i>Plate 4-1 Bridge geometry as observed on site.....</i>	<i>36</i>
<i>Plate 4-2 No hogging reinforcement in the slab, the concrete looks generally weak with a higher percentage of coarse materials.....</i>	<i>37</i>
<i>Plate 4-3 Bridge underside showing steel beams and pier.....</i>	<i>38</i>
<i>Plate 4-4 Manafwa River Bridge superstructure cross section immediately after the failure.....</i>	<i>38</i>
<i>Plate 4-5 Transverse cracks in deck surfacing and concrete patching.....</i>	<i>38</i>
<i>Plate 4-6 Opening in superstructure slab showing longitudinal steel beam, bottom reinforcement, disintegrated concrete layer and gravel layer under surfacing.....</i>	<i>39</i>
<i>Plate 4-7 Progressive failure of the deck slab with longitudinal cracks increasing in size till failure.....</i>	<i>50</i>
<i>Plate 4-8 Failed Deck Slab – design strength of 30MPa.....</i>	<i>51</i>
<i>Plate 4-9 Progressive failure of the deck during the testing with punching shear observed.....</i>	<i>51</i>
<i>Plate 4-10 Total failure of the deck slab indicating that punching shear behaviour observed in the 13MPa deck slab was the main cause of failure for this model.....</i>	<i>52</i>
<i>Plate 4-11 Failed Deck Slab – Indicates that the main cause of failure is punching shear regardless of the load but rather longitudinal cracking in the deck slab.....</i>	<i>53</i>
<i>Plate 4-12 Total deformations of the failed bridge element.....</i>	<i>55</i>
<i>Plate 4-13 Failure in the Model compared to the actual failure in the bridge deck slab.....</i>	<i>57</i>
<i>Plate 4-14 Bottom surface Failure of the Experimental model 13MPa deck slab vs Actual Bridge structure.....</i>	<i>58</i>

LIST OF TABLES

<i>Table 2-1 Studies undertaken on RC slabs to determine punching shear failure.....</i>	<i>14</i>
<i>Table 2-2 Field Experimentation tests of RC bridge deck slabs subjected to shear failure.....</i>	<i>15</i>
<i>Table 3-1 Correction factor for length to diameter ratios less than 1.75</i>	<i>27</i>
<i>Table 4-1 Punching shear capacity of existing superstructure slab for loading applied at the middle point of the slab.....</i>	<i>46</i>
<i>Table 4-2 Ultimate Limit State Sagging moment capacity of the Existing slab</i>	<i>47</i>
<i>Table 4-3 — Ultimate bending moment and shear forces in one-way spanning slabs.....</i>	<i>47</i>
<i>Table 4-4 Superstructure slab applied moments</i>	<i>47</i>

CHAPTER 1. INTRODUCTION

Uganda is bestowed with beautiful vegetation and wildlife, forests, water bodies and the sunshine that keep the environs and atmosphere cool all the year round. On the other hand, natural limitations to mobility and suppleness occur owing to Uganda's endowments. This is specifically true for all the lakes and rivers that oblige and give need to expensive bridges to enable manoeuvres and movements. The chapter gives a background to the thesis and explores the problem that necessitated the research to be undertaken. The thesis is defined by the main objective with specific objectives which were the basis of the different methods and materials used in the study but limited within the defined scope of works.

1.1 BACKGROUND TO THE STUDY

In Uganda majority of the bridges on the Uganda National Roads Authority (UNRA) network were constructed by the British during the colonial periods in the middle 20th century (from early 1930 to 1962). UNRA, the body charged with the national road network and bridges was established by an Act of Parliament in 2006 and is mandated with developing, expanding and maintaining the national roads network. From its establishment, many other bridges have been constructed in recent years especially on the district road network bridges and the national road network owing to the expansion of the road network. The bridges were designed to carry very low traffic loads yet they continue carrying loads that were not designed to carry.

Majority of the bridges are considered historically critical and significant, nevertheless, they are continually deteriorating in performance with many collapsing and hence reducing in number because of their degrading and unserviceable condition. Maintaining and conserving these bridges is quite a difficult task as many amongst them have materials and structural forms that are not related to the 21st-century bridges. An improved and better understanding of the materials utilized for the historic bridges and the structural behaviour and responses is very critical to the evaluation and preservation of these bridges.

1.2 STATEMENT OF THE RESEARCH PROBLEM

With an overall road network encompassing of over 20,000km of national roads, 13,000km of district roads, 2,800km of urban roads and 30,000km of community access roads, Uganda's motorway linkage has significantly increased and expanded. At the time of independence in 1962, the motorway road network comprised of about 400km. Uganda lays claim to having over 400 bridges, the majority of which were constructed using obsolete technology in the colonial periods when the country comprised of only about 5,000 vehicles (the biggest type being salon cars). The railway network at that point in time was the main means of transport for the heavy goods and raw materials used in the local industry for production. As such the bridges were mostly designed for accessibility and mobility, and thus there is need to assess the structural capacity and performance.

The bridges discussed above were built using mainly concrete, with some using timber.

With this in mind, it is possible that the structural capacity of these bridge may have been compromised. There was a build-up of over 120 bridges at the time of the study that urgently required replacement and/or repair to cope with the current traffic growth and axle load (Ogwang, 2012). Majority of the steel type bridges transferred to Uganda from the United Kingdom in the colonial era after use in the Second World War are collapsing or showing signs of failure attributed to fatigue-correlated damage. For instance, the Mitaano Bridge on the Rukungiri-Mitaano-Kanungu highway that connects Uganda to the Democratic Republic of Congo collapsed in 2012 under the weight of a trailer overloaded with 50 tons of cement as shown in Plate 1-1. The Aswa Bridge on the Lira-Pader border also collapsed (Plate 1-1 below) showing further the poor state of Bridges countrywide. The old bridge was constructed in 1936 at Puranga in Northern Uganda by the British colonialists. The trailer truck carrying over 30 tons of cement broke midway through the bridge and plunged into the river.



Plate 1-1 Collapse of the Mitooma Bridge and the Aswa Bridge respectively

Another bridge that collapsed in the recent years is the Manafwa Bridge constructed 60 years back and that is located in Busiu Sub County located in Mbale District which is shown in Plate 1-2. A part of the bridge located on the Mbale – Tororo Highway caved in leaving a very large hole in the middle of the bridge resulting into a paralysis of traffic along the road that links the Northern part of Uganda and Southern Sudan to the Central part of Uganda. Because of the collapse, traffic along the road was disturbed hence impacting on the economy significantly.



Plate 1-2 Failure of the Manafwa Historic bridge

A 55-year old bridge located in the city of Kiruna in Northern Sweden which was due for demolition mainly because of urban transformation was used by Bagge *et al.* (2014; 2015) to carry out tests on punching shear failure. The deck slab was tested by loading it in the middle of the span just close to the main girder that had not been damaged until there was a sudden shear failure that occurred. The failure was very similar to that of the Manafwa bridge. The methods undertaken for the bridge assessment included a desk study carried out on investigations done on the bridge previously by Nilimaa (2015), Nilimaa *et al.* (2016), Bagge & Elfgren (2016) and Huang *et al.* (2016). This research resembles the research work undertaken in this study.

1.3 RESEARCH OBJECTIVES

1.3.1 Main Objectives

The overall objective of this research is to investigate the structural characterisation and performance evaluation of the failed Manafwa historic bridge in Uganda.

1.3.2 Specific Objectives

The specific objectives of the research included the following:

- i. To determine the material and physical characteristics of the failed historic bridge
- ii. To numerically determine the structural performance of the historic bridge
- iii. To experimentally determine the structural failure mechanism and performance of the historic bridge part that leads to the failure of the bridge
- iv. To compare the numerical and the experimental performance results for the failed historic bridge.

1.4 SCOPE OF WORK

The research focused on structural characterisation aimed at the determination of the performance of the historic bridge. This was aided by the determination of the damage pattern and the conditional assessment of the bridge which information was based on in the recommendations to provide means through which the performance and longevity of the historic bridges can be enhanced. Numerical simulations were carried out using the information obtained from the material characterisation and the non-destructive tests carried out on the bridge to predict the failure mode of the bridge. The numerical simulation was carried out using a Finite Element Analysis of ANSYS. The critical part of the bridge which resulted in the failure was then modelled in the laboratory and tested for punching shear failure. The comparison of the results of the numerical simulation and the experimental model were then to draw a conclusion on the probable cause of failure of the historic bridge and recommendations made for further studies and means of improving the performance of the historic bridges in East Africa.

1.5 JUSTIFICATION

A new bridge is currently being constructed across the River Nile in Jinja. The bridge is constructed to replace the old Nalubale Bridge that was constructed and commissioned in 1954. Feasibility studies were conducted by the government of Uganda with funding

from the government of Japan to determine the suitability of the Old Nalubale Bridge. The findings of the studies and the field surveys indicated distinct deteriorations of the old bridge due to the ageing and could not rule out the possibility and danger of any spontaneous future collapse. The feasibility study report recommended that immediate repairs of the existing bridge were paramount or an alternative bridge constructed as soon as possible. Based on the findings of the report, there was validity for project implementation but does raise concerns with regards to other bridges that were constructed earlier or in the same time period of the Nalubale Bridge that is being reconstructed. A number of bridges have already collapsed leading to severe repercussions to the economy of the country and leading to loss of life.

There is a great need to study and forward means of evaluating the state in which most of the historic bridges are in and as a result put forth recommendations. The undertaking of this research study was also prompted by a number of factors, as described in the problem statement above that are summarized herewith;

- a) Changing Bridge construction practice all over the world in comparison to the local bridge practice
- b) Widespread damage, collapse and failure of Bridge structures and box culverts
- c) Lack of sufficient data to facilitate an engineering characterisation of the bridges constructed in the earlier years by the British during colonisation of Uganda
- d) Predicted urban population growth of the Uganda and high growth rates of the economy implying much higher traffic and the rise in the tonnage and quantities of loads (axle loads) being carried. Also, the Southern Sudan autonomy and discovery of oil and other mineral resources in different parts of Uganda have subjected the bridges to much more stress
- e) Predicted growth of services and industrial activities in the country

The research on the failure of bridges is the first to be undertaken at PAUSTI, it therefore is a good opportunity for all those enrolling in the course to undertake further research on the topic. The findings and the recommendations form good input to the implementing agencies charged with construction of bridges and their respective maintenance in the East African Community where many historic bridges are still functional.

CHAPTER 2. LITERATURE REVIEW

2.1 INTRODUCTION – BRIDGE TYPES AND CHARACTERISTICS

Bridges have been part of a human settlement for thousands of years. Historic bridges stand as evidence of the power and influence of past societies. They vary greatly in style and reflect the culture and engineering innovation of their society. The improvement of the performance and efficiency of bridges is a constant task of engineering design. Recent developments in concrete material properties have renewed the research interest for this topic (Muttoni, & Fernandez, 2008). In the context of this research, efficient structures are defined as structures that satisfy the design requirements with a minimum amount of materials, enabling easy and rational construction. Existing structures are investigated to identify the most successful shapes combining these properties. Structural analysis of bridges is a process to analyze a structural system to predict its responses and behaviors by using physical laws and mathematical equations. The main objective of structural analysis is to determine internal forces, stresses and deformations of structures under various load effects (Plos, et al, 2016).

Types of bridges include the following:

2.1.1 Simply supported Beam/Girder bridges

These consist of horizontal beams and/or girders that are simply supported (also referred to as pinned) at each end by piers (also known as columns) or abutments (bridge landing end supports) depending on the span. In consideration of structural analysis, the longer the spans of this type of beam, the weaker the structure becomes (Luttrell, 1987).

Beam bridges are the simplest and most basic type of bridge constructed and they rarely span more than 75 meter. The Manafwa bridge which is considered in this study is a simply supported beam bridge. There are two common types of girders; I beam and Box girder. Box plate Girder give increased stability and resistance, plus use for longer bridges while traversing curves. The Beam/I-Girder bridges are simple to design, applicable in very many different conditions and they are easy to fabricate (Tonias, & Zhao, 2018).



Figure 2-1 Simply supported I-girder bridge structure

2.1.2 Arch bridge

An arch bridge is a semicircular pined structure with abutments on each end. Depending on the structural material it can be either an RC arch bridge or a steel truss arch bridge. The design of the arch is such that the load is carried outward along two paths curving towards the ground by compression. The greater the degree of curvature, the greater the effect of compression. Arch bridges are made of steel or concrete and they can span up to 800 feet (240m) depending on the structural form and material. However beam/girder bridge, effects of span will eventually overtake the natural strength of the arch (Chen & Duan, 1999).



Figure 2-2 The Old Trails Arch Bridge

2.1.3 The suspension bridge

Suspension bridge is one where cables (wire strands/ ropes/chain) are strung across the river or whatever the obstacle and the deck is suspended from there cables. The M type of suspended bridge is one were cables are slung through/over tall towers. Another form of a suspension bridge is the cable stayed bridge. As opposed to the M shaped suspension bridge, cable stayed bridge has an A shaped form, in which the cables are run from the roadway up to a single tower, where they are secured. The deck is suspended by the cables over the tower (Chen & Duan, 1999).



Figure 2-3 Nile River suspension bridge being constructed in Uganda

2.1.4 Steel truss bridges

Truss bridges are an assembly of steel section in triangulations to form truss Girders/, lattice girders or open web girders. They are efficient and economical structural systems, since the members experience essentially axial forces and hence the material is fully utilized. Members of the truss girder bridges can be classified as chord members and web members. Generally, the chord members resist overall bending moment in the form of direct tension and compression and web members carry the shear force in the form of direct tension or compression. Due to their efficiency, truss bridges are built over wide range of spans. They are generally used for bridge spans between 30m and 150m where the construction depth (deck soffit to road level) is limited (Tonias, & Zhao, 2018).

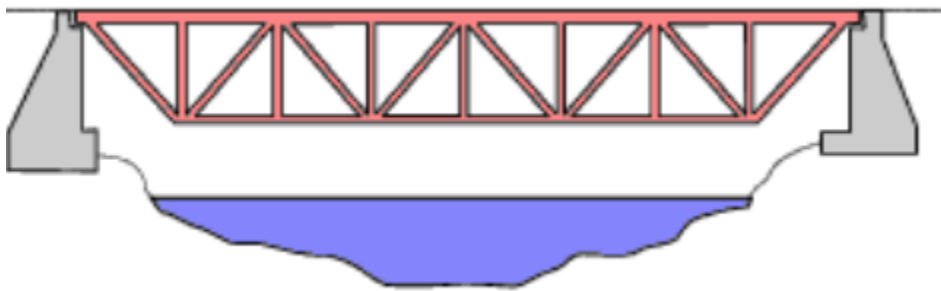


Figure 2-4 Steel Truss bridge layout

2.1.5 Types of bridge decks

All bridge types carry a deck of one form or another. The deck implies the superstructure part of the bridge (slab and its supportive system). It can be either a pure RC deck or a composite type with different forms of structural strengthening (Luttrell, 1987). The types of bridge decks are explained here-under.

2.1.5.1 Cast in-situ reinforced concrete decks

The three most common types of reinforced concrete bridge decks are the solid, voided and beam slab which are shown in the pictures below. Solid slab bridge decks are the most useful for small, single or multi-span bridges and are easily adaptable for high skew. Voided slab and beam and slab bridge decks are used for larger, single or multi-span bridges (Kudzys, 1999).



Figure 2-5 Solid Slab

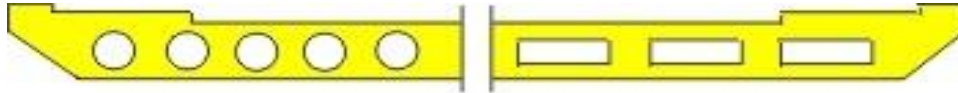


Figure 2-6 Voided Slab

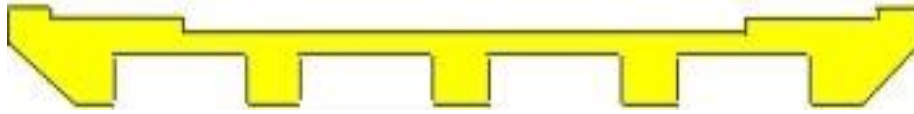


Figure 2-7 Beam and Slab

2.1.5.2 Pre-stressed concrete decks (often pre-cast)

These comprise Pre-tensioned beams with in-situ concrete deck (voided or solid) and Post-tensioned concrete beams with in-situ concrete deck (voided or solid). The term pre-tensioning is used to describe a method of pre-stressing in which the tendons are tensioned before the concrete is placed, and the pre-stress is transferred to the concrete when suitable compressive strength is reached. Post-tensioning is a method of pre-stressing in which the tendon is tensioned after the concrete has reached a suitable strength (Chen, 1999).

2.1.5.3 Composite decks

Composite bridge decks refer to all decks designed and constructed in such a way that there is interaction in load transfer between in-situ reinforced concrete (usually the slab deck) and structural steel (Luttrell, 1987). The three main economic advantages of composite construction include smaller depth of beam, reduced cross-sectional area of the steel top flange and reduction in transverse stiffening for the top compression flange of the steel beam can be reduced because the restraint against buckling is provided by the concrete deck. The Manafwa bridge is a composite deck type.



Figure 2-8 Typical composite deck

2.2 BRIDGE STRUCTURAL ANALYSIS

2.2.1 Common structural and material defects (concrete) in bridge structures

Concrete is used in structures as mass concrete or normally it is combined with steel reinforcement or with prestressing steel. Defects in concrete are often related to the lack of durability resulting from the composition of the concrete, poor placement practices, poor quality control, insufficient curing or the aggressive environment in which it is placed (Wang, 2006).

- a) **Cracking:** It is recognised that in reinforced concrete, cracks will form in tension zones. These fine structural cracks are considered harmless but as reinforcement is further stressed the initial cracks open up and progressively spread to longer and wider cracks. Further cracking can result in blocks forming and at this stage a detailed inspection is required. Cracks should be photographed to enable historical recording of crack propagation and growth.
- b) **Spalling:** A spall is a fragment of concrete detached from the structure between fracture surfaces. Spalling is a continuation of the corrosion process and represents a serious defect in the concrete, in that the reinforcement is heavily corroded.
- c) **Delamination:** Delamination is defined as a discontinuity in the surface concrete which is substantially separated but not completely detached from the adjoining concrete. Visibly it may appear as a solid surface but can be identified by the hollow sound when tapping with a light hammer. Delamination generally begins with the corrosion of reinforcement and subsequent cracking of the concrete parallel to the exterior surface.
- d) **Patching or Other Repairs:** The condition of the repair or patch will indicate whether the underlying problem has been solved or if it has been merely covered up and is actively continuing under the repair. Cracking, delamination, rust stains or spalling around the patch indicates the problem still exists and further investigations and repairs are needed.
- e) **Corrosion of Reinforcement:** The concrete alkalinity protects the reinforcement from corrosion but when moisture, air and/or chloride ions above a certain concentration penetrate through the concrete to the reinforcement, this protection breaks down and corrosion commences. In the initial stages, corrosion may appear as rust stains on the concrete surface. In the advanced stages, the surface concrete cracks, delaminates and spalls exposing heavily corroded reinforcement. Spalling and delamination are indications of advanced corrosion. In prestressed concrete structures, any indication of corroding prestressing steel is very serious as the failure of the strand or wire may lead to a non-ductile or catastrophic failure of the component.

2.2.2 Non Destructive Testing of Bridge

It is often necessary to test concrete structures after the concrete has hardened to determine whether the structure is suitable for its designed use. Ideally such testing should be done without damaging the concrete. The tests available for testing concrete

range from the completely non-destructive, where there is no damage to the concrete, through those where the concrete surface is slightly damaged, to partially destructive tests, such as core tests and pull out, where the surface has to be repaired after the test (Seshu & Murthy, 2013).

The testing of existing structures is usually related to an assessment of structural integrity or adequacy. In either case, if destructive testing alone is used, for instance, by removing cores for compression testing, the cost of coring and testing may only allow a relatively small number of tests to be carried out on a large structure which may be misleading. Non-destructive testing can be used in those situations as a preliminary to subsequent coring (Seshu et al, 2013).

Typical situations where non-destructive testing may be useful include (Murthy, 2013):

- i). Quality control of pre-cast units or construction in situ
- ii). Removing uncertainties about the acceptability of the material supplied owing to apparent non-compliance with specification
- iii). Confirming or negating doubt concerning the workmanship involved in batching, mixing, placing, compacting or curing of concrete
- iv). Monitoring of strength development in relation to formwork removal, cessation of curing, prestressing, load application or similar purpose
- v). Location and determination of the extent of cracks, voids, honeycombing and similar defects within a concrete structure
- vi). Determining the concrete uniformity, possibly preliminary to core cutting, load testing or other more expensive or disruptive tests
- vii). Determining the position, quantity or condition of reinforcement
- viii). Increasing the confidence level of a smaller number of destructive tests

The following methods, with some typical applications, have been used for the non-destructive testing of concrete (Shetty, 2010):

- 1) Visual inspection, which is an essential precursor to any intended non-destructive test to establish the possible cause(s) of damage to a concrete structure and hence identify which of the various NDT methods available could be most useful for any further investigation of the problem.
- 2) Half-cell electrical potential method, used to detect the corrosion potential of reinforcing bars in concrete.
- 3) Schmidt/rebound hammer test, used to evaluate the surface hardness of concrete.
- 4) Carbonation depth measurement test, used to determine whether moisture has reached the depth of the reinforcing bars and hence corrosion may be occurring.
- 5) Permeability test, used to measure the flow of water through the concrete.
- 6) Penetration resistance or Windsor probe test, used to measure the surface hardness and hence the strength of the surface and near surface layers of the concrete.
- 7) Covermeter testing, used to measure the distance of steel reinforcing bars beneath the surface of the concrete and also possibly to measure diameter of the reinforcing bars.

- 8) Radiographic testing, used to detect voids in the concrete.
- 9) Ultrasonic pulse velocity testing, mainly used to measure the sound velocity of the concrete and hence the compressive strength of the concrete.
- 10) Sonic methods using an instrumented hammer providing both sonic echo and transmission methods.
- 11) Impact echo testing, used to detect voids, delamination and other anomalies in concrete.
- 12) Ground penetrating radar or impulse radar testing, used to detect the position of reinforcing bars or stressing ducts.
- 13) Infrared thermography, used to detect voids, delamination and other anomalies in concrete and also detect water entry points in buildings.

Additionally, any one of the following tests will be used depending on the availability in cases where the three above methods are not sufficient to determination of all the parameters required for the Research.

2.2.3 Schmidt Rebound Hammer Test

The Schmidt rebound hammer is principally a surface hardness tester. It works on the principle that the rebound of an elastic mass depends on the hardness of the surface against which the mass impinges. There is little apparent theoretical relationship between the strength of concrete and the rebound number of the hammer. However, within limits, empirical correlations have been established between strength properties and the rebound number (Troxell et al, 2018).

2.2.4 Core Test

In most structural investigations or diagnoses extraction of core samples is unavoidable and often essential. Cores are usually extracted by drilling using a diamond tipped core cutter cooled with water. Broken samples, for example, due to popping, spalling and delamination, are also commonly retrieved for further analysis as these samples may provide additional evidence as to the cause of distress. The selection of the locations for extraction of core samples is made after non-destructive testing which can give guidance on the most suitable sampling areas. For instance, a cover meter can be used to ensure there are no reinforcing bars where the core is to be taken; or the ultrasonic pulse velocity test can be used to establish the areas of maximum and minimum pulse velocity that could indicate the highest and lowest compressive strength areas in the structure (Tur, and Derechennik 2018).

Moreover, using non-destructive tests, the number of cores that need to be taken can be reduced or minimized. This is often an advantage since coring is frequently viewed as being destructive. Also the cost of extracting cores is quite high and the damage to the concrete is severe. The extracted cores can be subjected to a series of tests and serve multiple functions such as: confirming the findings of the non-destructive test, identifying the presence of deleterious matter in the concrete, ascertaining the strength of the concrete for design purposes, predicting the potential durability of the concrete and

confirming the mix composition of the concrete for dispute resolution (Tur, and Derechennik 2018).

2.3 STRUCTURAL RESPONSE OF REINFORCED CONCRETE SLABS

The majority of bridges all over the world are made up of reinforced concrete slabs (referred to as RC slabs in the thesis). As a result, many research projects in different universities all over the world have been conducted in a bid to understand and conceptualize the actual structural behavioral patterns of the RC slabs. Shahrooz (1994) and Amir (2014) carried out research for RC slabs by subjecting them to different failure mechanisms following design and assessment methods that are all incorporated into building codes used for engineering practice. Increasing technological innovations due to the development of computers and software have resulted into determination of Finite Element Methods (referred to as FEM) and many software that are key in assessing the failure responses and patterns of the RC slabs (Zheng et al. 2009, Eder et al., 2010 and Belletti et al. 2014).

2.3.1 Failure Modes

When reinforced concrete slabs that have no shear reinforcement are loading with a point load or a concentrated load, they fail in three mechanisms namely; Bending failure, Shear and Anchorage failure. Of the three failure mechanisms, the bending failure is the preferred failure mode. This is because during bending failure, the structure undergoes ductile deformation and then redistribution of the internal forces and moments before it eventually collapses. On the contrast, shear failure is not desired for the deck slabs as it is a brittle failure that results into an unexpected collapse of the structure before ductile deformation takes place. Consequently, when shear failure takes place, it will result into much more losses and damage to both property and human life making it a lot more dangerous than the other failure modes (Muttoni, & Fernandez, 2008).

The most common failure mode is the shear failure mechanism. Review of literature done indicates that there are two different types of shear failure. They include one-way shear failure and two-way shear failure which is commonly referred to as punching shear failure. One-way shear failure takes place when the slab system is loaded by a line load and/or has line boundary conditions for its support. An example of the one-way shear failure takes place in slab-wall systems. Punching shear failure (will be used in the Thesis instead of two-way shear failure) takes place when the slab is loaded with a concentrated load or supported which is then spread out onto the entire slab. Common examples of punching shear failure are encountered in slab – column systems (Zandi, 2016)

The third failure mechanism, anchorage failure, is not very common but occurs as a result of bond-slippage between the concrete and the reinforcements. However, the anchorage failure mode was not considered in the research carried out by (Shu, J., 2016) because no signs were encountered to indicate that slippage was encountered in the deck slab and additionally, the deck slab had fixed supports to permit any anchorage failure to take place. Anchorage failure considering bond-slip between reinforcement and concrete is another common failure mode for RC structures. However, this failure mode is not the

major concern in this study because no signs of slippage were encountered and the deck slab was fixed in position to enable any anchorage failure (Zandi, 2016).

2.3.2 Punching shear failure mechanism

The term punching shear as described above occurs when a slab (reinforced concrete or normal concrete slab) is loaded with a concentrated load which exceeds the slab capacity. The shear force distributed per unit length when punching shear is taking place becomes very high in the proximity of the loading area. Punching shear failure may occur within the discontinuity regions if the ability of the slab punching shear is exceeded (Owilli, 2017). A punching shear failure mechanism occurs when the compression region around the concentrated force fails as a result of the concrete strain attaining a critical level. The failure is as a result of combined action of both flexural and shear loading leading to a combination of flexural tangential and bending and inclined shear cracking as shown in Figure 2-1 and 2-2 below. From Hallgren in 1996 (Amir 2014), shear failure occurs when the tangential compression strain in the slab at the edge of the compressive load reaches a critical value. This weakens the concrete at the edge where the compressive load is acting until a critical value is reached leading to failure (Owilli, 2017).

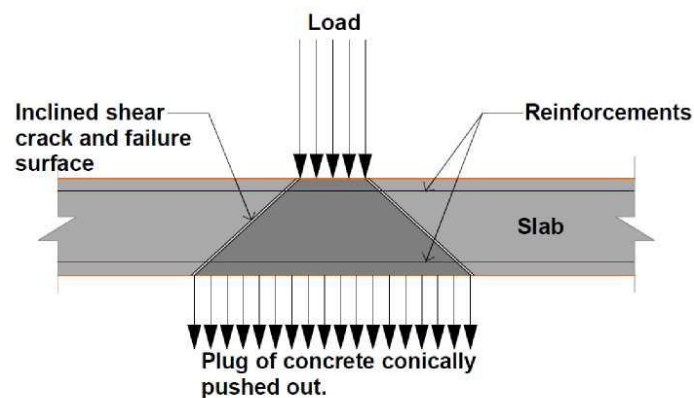


Figure 2-9 Punching shear failure section in concrete deck due to concentrated load

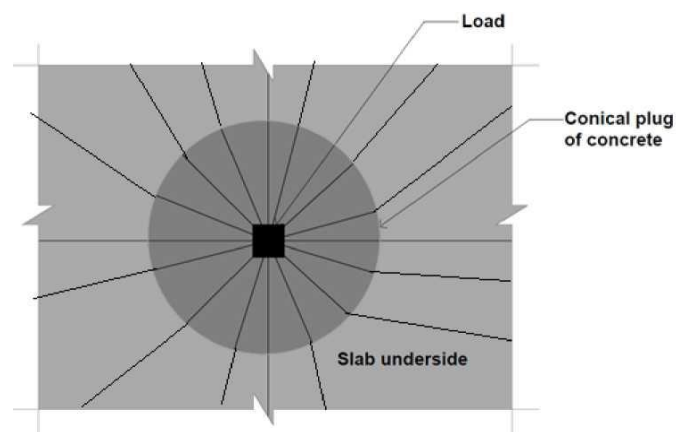


Figure 2-10 Punching shear failure on the underside of the bridge deck due to concentrated load

In bridge deck slabs, the punching shear mechanism described in section 2.2.2 is not truly

symmetrical since the flow of inner forces varies quite significantly from that observed in slab-column specimens. The transverse spans are much smaller than the longitudinal spans, this is the case in the Manafwa bridge. The transverse span (distance between the two girders) was 1400m compared to the longitudinal span of 10m (span between the abutment and the piers). And the radial cracking lines can be long and sometimes may not even be visible on the underside of the slab depending on the aspect ratio (Owilli, 2017).

2.3.3 Review of research carried out and experimental model for reinforced concrete slabs

The table 2-1 below summarizes the different reviews and studies undertaken on RC Slabs while carrying out assessments for punching shear failure.

Table 2-1 Studies undertaken on RC slabs to determine punching shear failure

Talbot (1913)	<ul style="list-style-type: none"> Carried out tests on 200 foundation footings for both walls and columns, and the results indicated that 20 footings failed in punching shear. The research proposed a simple model to enable determination of the critical shear stress subjected around a circumference of the concentrated load
Kinnunen & Nylander (1960)	<ul style="list-style-type: none"> Tests on 61 circular slabs were executed with circular columns, varying flexural reinforcement ratio. The results were used to form a calculation method for punching shear. An assumption was taken that for a given critical rotation, the punching capacity of the circular slabs was reached.
Moe (1961)	<ul style="list-style-type: none"> The research included tests on square slabs to punching failure. Consequently, a limit state model was proposed (using mechanical and empirical relation) It was assumed that shear stress limitation was reached at a critical perimeter with a given distance to the loading area. The study was based on to formulate the ACI-Standard 318 of the year 1963 which over the years has been improved.
Muttoni (2009)	<ul style="list-style-type: none"> Proposed punching failure criterion by The study proposed an assumption that two-way shear depends on the extent of rotation of the slab. A comparison of test results of the Critical Shear Crack Theory was done with experiment results of 99 tests obtained from literature.

Muttoni (2003)	<ul style="list-style-type: none"> • Carried out 253 shear tests in the study • Formulated the Critical Shear Crack Theory basing on the results of the 253 shear tests done. • The study assumed that shear strength was directly dependent on the extent of the roughness and the width of the “Critical Shear Crack”.
----------------	---

2.3.4 Field Test of a Bridge Deck Slab

From the literature review carried out, it is quite evident that very few field tests have been carried out on in-situ (real) bridge deck slabs. In Table 2-2 below, the field tests conducted on reinforced concrete deck slabs are summarized in the table below that were subjected to shear through use of vehicular wheel loads and consequently failed by punching shear.

Table 2-2 Field Experimentation tests of RC bridge deck slabs subjected to shear failure.

Miller <i>et al.</i> (1994)	<ul style="list-style-type: none"> • Miller conducted multiple tests on the deck slab until of a 38 year old bridge that had been abandoned to the point of failure. • The bridge portrayed vast similarities with the Manafwa bridge as the concrete in the shoulder area should signs of deterioration and the reinforcement bars were exposed and as such should signs of corrosion. • The bridge failed in shear after being subjected to concentrated loads. However, it did not reach its theoretical bending capacity.
Pressley <i>et al.</i> (2004)	<ul style="list-style-type: none"> • Conducted two destructive bending tests and two destructive punching shear tests on a 33-year old Reinforced Concrete flat slab bridge “No 1049”. • The results indicated that in order to attain maximum load carrying capacity and load distribution of the deck slab to maximumly bear the punching shear, the pile-soil interactions needed to be modelled.
Lantsoght <i>et al.</i> (2016)	<ul style="list-style-type: none"> • Lantsoghth carried out a number of tests on an old reinforced concrete slab bridge (which was 42 years old at the time of testing) and is located on the “N924” highway in Sweden. • The results indicated that the bridge failed in bending yet the theoretical computations based on Eurocode 2 estimated that

the bridge would fail in punching shear.

- Furthermore the study concentrated on determining the contribution of the type of reinforcement bars (smooth reinforcement bars versus ribbed reinforcement bars) and as such cut the bridge deck slab into a number of beams that were tested in the laboratory.

2.3.4.1 *Non-Destructive Testing of Bridge*

Concrete structures often need to be tested when the concrete has hardened over the years to be able to ascertain if the concrete meets the design parameters and is suitable for use. The testing must not be destructive to the structure for the continued use of the structure. As such non-destructive testing is a very important attribute for concrete structures (Miller, et al, 1994). Many tests have been developed and they range from those that are non-destructive (where no damage whatsoever to the concrete takes place), to those that are partially destructive (concrete surface is distorted and/or slightly damaged while carrying out the test) and to those that very destructive. Some of the partially destructive tests include the coring test which was also used in this study, pull-out and pull-off tests. In these tests, the concrete surface is always repaired after the test is done (Seshu & Murthy, 2013).

There is always need to determine the structural performance and integrity of existing structures and as such the testing of these parameters must be carried out especially when the design life of the structure is done or when signs of deterioration are observed. For determination of the structural integrity or adequacy of the structure, destructive testing alone is not sufficient to determine this. This is because the destructive testing is limited and as such only a small number of tests can be carried. For instance if core testing is to be used on a large structure, few cores will be taken as the cost of coring and testing is high and the work is very laborious. The results consequently may be misleading. From this, it is therefore important for non-destructive testing to be carried out as a preliminary testing measure, upon which subsequent coring can be planned and carried out for the areas of weakness as indicated by the non-destructive testing (Seshu & Murthy, 2013).

2.3.4.2 *Schmidt's Rebound Hammer Test*

The objective of using the Schmidt Rebound hammer method was to assess the compressive strength of concrete with the help of suitable co-relations between rebound index and compressive strength of the superstructure (deck slab and parapet wall) and substructure (piers, abutments and the footing). As such, it was also possible to assess the uniformity of the concrete, and the quality of the concrete in one element in relation to the standard requirements and concrete in other areas (Seshu, & Murthy, 2013). The test was used based on the principle that the rebound of the elastic mass in the hammer depends upon the relative hardness of the surface that it is used against. As such, each time the plunger of the hammer was pressed against the concrete surface, the mass rebounded and the extent of the rebound depended on the surface hardness which is a

relative measure of the compressive strength of the concrete. Thus, a low strength low stiffness concrete will absorb more energy than high strength concrete and will give a lower rebound number (Miller, et al, 1994).

2.4 FINITE ELEMENT METHOD

2.4.1 The finite element method and element formulations

The finite element method (FEM) is a general tool for solving differential equations necessary in applications of structural engineering. FEM has the capability of handling large and or complex structural modelling mechanics challenges and problems by use of discretization processes into a number of many finite elements, which in turn is governed by the element and global equations. Since the element equations govern the model and the results, it is important that designers have a fair understanding of the underlying assumptions of these elements (Klein, 2006). An example of an FEM model is shown in Figure 2-3 below.

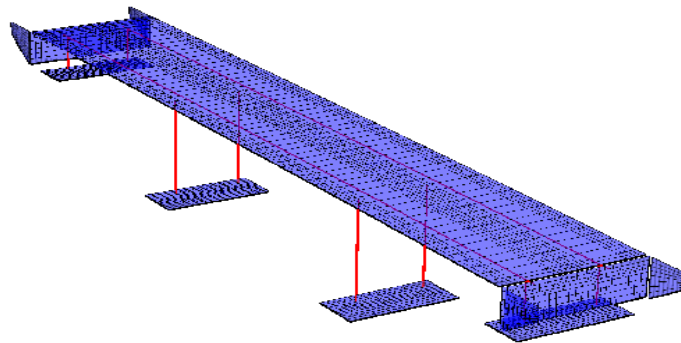


Figure 2-11 Example of finite element structural analysis model of a double beam bridge

2.4.2 Finite element modelling and analysis of reinforced-concrete bridge decks

Despite its long history, the finite element method continues to be the predominant strategy employed by engineers to conduct the structural analysis. The primary objective of this study was to establish and demonstrate a convenient, reliable, and accurate methodology for analysing reinforced-concrete structures with particular emphasis on reinforced-concrete bridge decks. A secondary objective was to develop a capability for predicting stress and strain distribution through the thickness of reinforced concrete bridge decks. Such information is not easily obtained through experimentation (Biggs, et al, 2000).

In a study by Seshu, & Murthy (2013), ANSYS software which is a general-purpose finite element code) was used to perform analytical evaluations. The results from the software depicted non-linear behaviour and patterns of concrete. The software also showed vast capabilities to describe the behaviour of the constituent reinforcement bars in the concrete independently of the mass concrete material. ANSYS was also used to develop three-dimensional models (finite element models) that were based on to determine the overall response and structural assessment of different RC systems. The software was also used to determine bi-axial strain distributions of the models through the element thickness. Displacements and strain patterns in the element were predicted

with a high accuracy degree. The accuracy of the results of the modelling were verified using o theoretical calculations and using response data from the laboratory testing that was carried out.

Basing on these models that were developed, Seshu (2013) was able to evaluate the structural integrity of the Route 621 Bridge located on the Willis River. Similarly to the study undertaken in this thesis, the software was used to determine the global response of the steel girders and the RC deck slab. The reason why ANSYS was used for this research is because it was used before as in this study and yielded positive results which were verified and found consistent.

2.4.3 Finite element modelling and analysis using ABACUS

Biggs, Gomez and McKeel carried out a study to establish and demonstrate a convenient, reliable, and accurate methodology for analysing reinforced-concrete structures with particular emphasis on reinforced-concrete bridge decks in 2000. A secondary objective was to develop a capability for predicting stress and strain distribution through the thickness of reinforced concrete bridge decks. Such information is not easily obtained through experimentation. A specific objective of the analytical evaluation included the development of a finite element model that could correctly represent global bridge behaviour and accurately predict strains, stresses, and displacements in the deck. Dynamic, fatigue, and thermal analyses, although certainly worth investigating in future project phases, were not included in this study (Biggs, Barton et al, 2000)

Analytical evaluations were performed with the commercial, general-purpose finite element code ABAQUS, which can effectively depict the nonlinear behaviour of concrete. It also has the unique capability of describing the behaviour of reinforcing bars independently of the concrete material. Three-dimensional finite element models were developed to determine the overall structural response of several reinforced-concrete systems. Biaxial strain distribution through the element thickness, longitudinal normal girder strains, and displacements were predicted with reasonable accuracy. The accuracy of the model was verified with hand calculations or response data acquired from laboratory testing. The validated finite element models of the structural systems were used to evaluate the Route 621 Bridge over the Willis River, specifically, the composite action and global response of the reinforced-concrete deck and steel girders.

2.4.4 Numerical Modelling and Validation of Composite Bridge Decking

In a study by O'Connor in 2013, Deck panels were made by combining consistent-quality pultruded subcomponents with a vacuum-infused outer wrap. The strength and stiffness were first determined analytically using finite element methods, then validated independently with extensive full-scale laboratory testing. Load testing further added to the calibration of the finite element model, so there was a high level of confidence that the numerical model was reliable. The study was mainly aiming at ascertaining and indicating the performance of lightweight decks on moveable bridges, historic bridges, and other structures that were not designed for heavy concrete decks. Many existing bridges were built with open steel grating, but long-term durability of the deck has been a

maintenance problem because of corrosion and fatigue cracking. Furthermore, there was testing of subcomponents and full-scale structural panels to validate finite models, and the installation and evaluation of the installation procedures. The project also entailed a finite element analysis of the bridge stringers and the complete deck system plus the railing system (O'Connor, 2013).

The first step included surveying the available materials and hence forth coming up with a light weight FRP deck system. The process used involved the first phase that entailed development of a design report on the selection of the suitable materials for use in the deck structure. The Deck system installed was subjected to moving traffic load tests so as to determine the load capacity of the bridge; which in most cases is not used or needed to assess the deck as indicated in the figure below. The purpose of the live-load testing was to enable collection of data (i.e. strains and deflections) on the performance of the FRP bridge deck that was installed in Bolivar, NY. The information was then used to complement the information that was derived from the finite element model. The finite element model used property values that were primarily derived from the physical testing of the as-fabricated composite specimens (O'Connor, 2013).



Plate 2-1 Traffic load tests to determine load capacity of composite decking

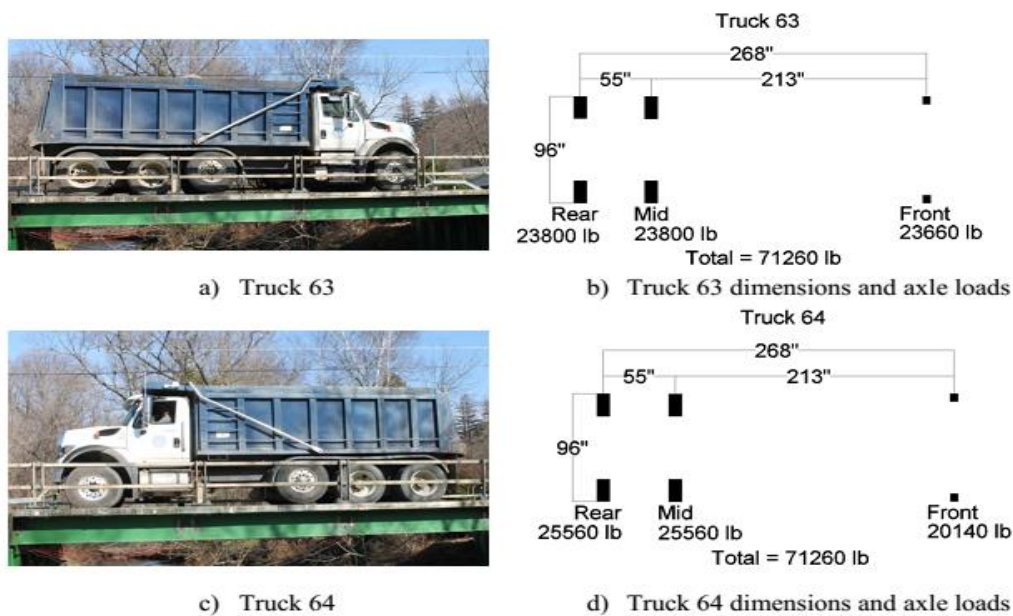


Figure 2-12 7600 tri-axle dump trucks used for live-load test.

From the Finite Element Analysis software, the following plots were obtained that may also be obtained in this research.

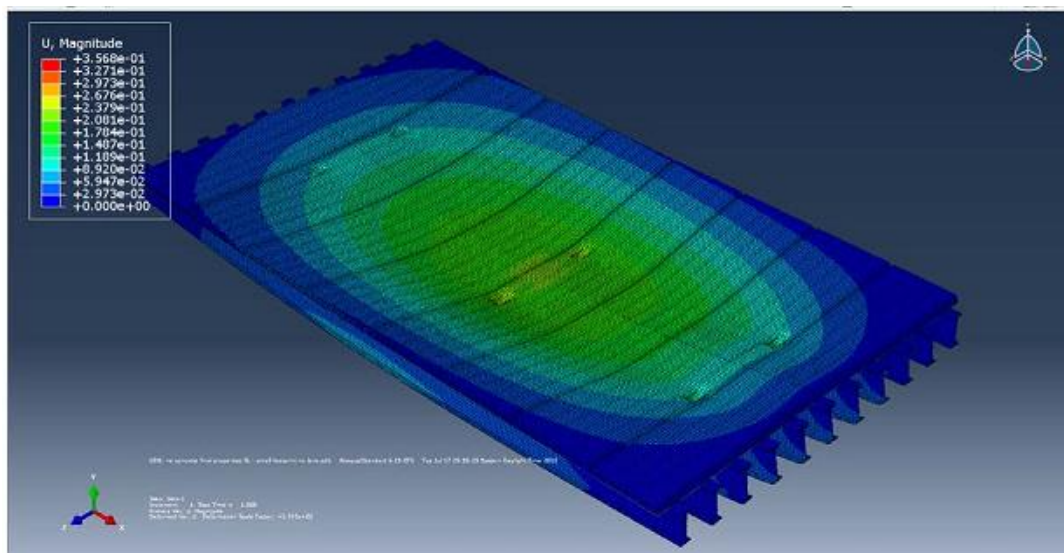


Figure 2-13 Service load deflection

The most critical element (the element with the highest Tsai Hill index under LRFD loading) was obtained as the one located under the area of applying the truck load (on the top flange).

Experimental Validation: Numerous laboratory tests were performed and information collected about the behaviour and consistency of tube subcomponents and full depth deck panels. Connections, the railing anchorage, the wearing surface, and fire resistance were also proof tested. The field testing was done to validate the finite element analysis. The live load test showed that the maximum tensile strains experienced by the FRP deck under the truck loading were below 3 percent of the ultimate failure tensile strain of the

FRP panel ($315 \mu\epsilon$) and that maximum mid-span deflections registered by the steel girders and FRP deck satisfy AASHTO deflection limits.

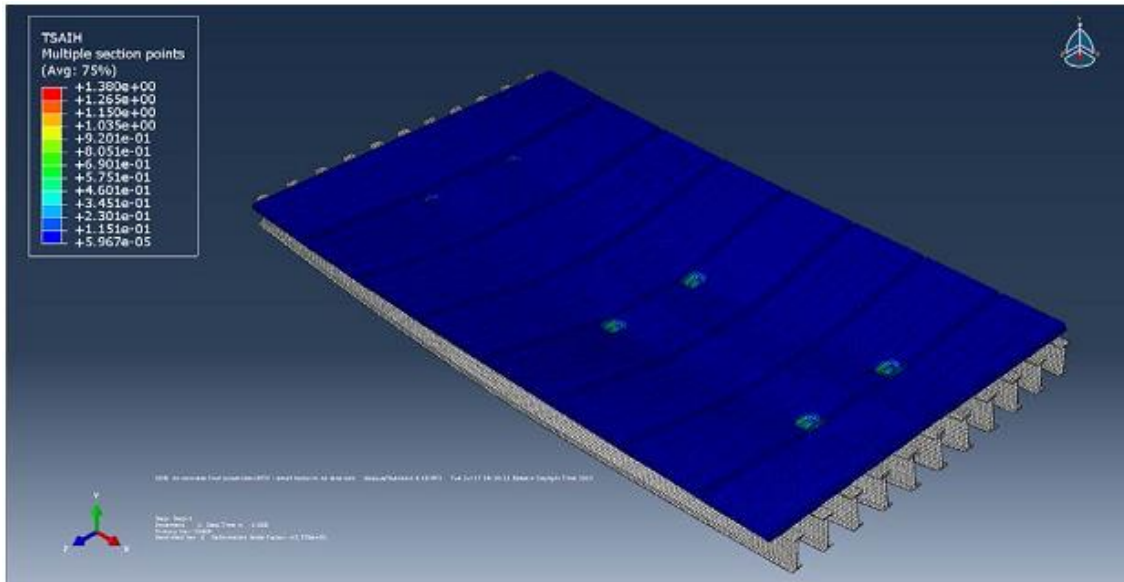


Figure 2-14 Tsai-Hill Index (R) ($\sqrt{I_{TH}}$) (LRFD)

The 3D finite element model was used to further evaluate the response of the FRP deck and steel girders to the truck loading. Numerical results matched very closely the experimental data. For example, for the load case of both trucks placed at mid-span, differences between the measured strain values on the FRP deck and the numerical model were on the order of 5 percent, whereas differences in steel girder deflections are on the order of 4 percent (O'Connor, 2013).

2.4.5 Finite element analysis of a composite bridge deck

During a very similar study by Klein in which he carried out a finite element analysis of a composite bridge in 2006, the complex nonlinear properties of concrete make it difficult to determine its true strength and response under loading conditions. As is encountered in many applications, it has often lead to many reinforced concrete structures such as bridge decks being over designed. Finite element analysis techniques such as the smeared crack approach exist to enable modelling of concrete structures with considerable accuracy. As such, the dissertation used the general purpose finite element software ABAQUS to model a composite bridge deck that comprises of a reinforced concrete slab and longitudinal steel girders. Three separate models were produced with different girder spacing. Loading conditions were then determined from the Australian Standard for Bridge Design and used on the structure to produce the worst effects. The response of the bridge deck was determined and an optimum girder spacing chosen. It was found that a four girder bridge deck would provide the optimum design for a two lane bridge to meet Australian Standards (Klein, 2006).

Results obtained showed that all models were able to withstand the stresses generated in their members. The exception was the girders at the supports as the boundary conditions did not represent an elastomer bearing pad. This caused excessive stress concentrations.

Both three and four girder bridges exceed the deflection limits for serviceability requirements making them unsuitable designs. The optimum girder spacing chosen was the four girder model for a two lane bridge to meet Australian Standards. Even though this did not meet deflection requirements it proved the most efficient design with the use of its materials. The maximum deflection was only slightly larger than the limit so it could be easily improved by increasing the girder size (Klein, 2006). There are a number of areas of this project where further work could be conducted and as such in carrying out this research, these areas will be given attention:

- i. The supports for the girders were modelled as if they were fixed to a completely rigid structure. This caused excessive stresses in the girders at these locations. Elastomer bearing pads could be modelled at these locations. This would remove the localised stresses on the girders and it would also be useful to find out how effective a typical bearing pad is at providing a smooth transition of stress from the girders to the supports.
- ii. The nonlinear geometry of the structure was not analysed with the models, therefore buckling effects were not considered. Nonlinear geometry could be used to ensure the separate models analysed are not subjected to these buckling effects.
- iii. The four girder bridge deck was chosen as being the optimum girder spacing. However, the deck was well over designed with very small stress values recorded in the reinforcement and in the concrete. Additional trial models could be produced with varying deck thicknesses and reinforcement areas. This would allow the optimum deck thickness for the four girder bridge-deck to be determined.

2.5 RESEARCH GAP – MANAFWA BRIDGE COMPARISONS TO TESTED BRIDGES

Tests on punching shear failure were carried out by Bagge *et al.* (2014; 2015) on a 55-year old bridge located in the city of Kiruna in Northern Sweden which was due for demolition mainly because of urban transformation (and not because it had deteriorated). The processes and methods undertaken for the bridge assessment involved carrying out of a desk study encompassing all investigations done on the bridge previously by Nilimaa (2015), Nilimaa *et al.* (2016), and Huang *et al.* (2016). Further, conditional study and destructive tests were conducted on the bridge before its eventual demolition. The research is very similar to the study undertaken in this research for the Manafwa Bridge. Whereas investigations had been carried out on this bridge and documented, no studies have been done on the Manafwa bridge prior to its eventual collapse.

The study provided the geometry (including the dimensions and the configuration) of the bridge which are shown in the figure 2-1 below. The research was undertaken in this thesis also sought to determine the configurations and dimensions which entails the physical characterization of the bridge. The study done by Bagge *et al.* (2014; 2015) entailed the bridge being tested to failure in between two of the main girders which closely resembles the actual failure of the Manafwa bridge. The deck slab was thereafter tested by loading it in the middle of the bridge span just close to the main girder that had

not been damaged until there was a sudden shear failure that occurred.

The figure 2-2 below indicates the extent of failure that resulted after the test was conducted. Punching shear type failure which is similar to the type of failure in the Manafwa bridge occurred next to plate 1 only, and not at plate 2. The researcher further indicated that observations on the underside of the tested slab (bottom part) pointed to a semi-circular failure under plate 1 which confirmed that shear failure had taken place on one side of the slab and consequently deduced that it was not pure punching failure ACI. (2014). The research in this research was undertaken to also ascertain the possibility of similar nature of failure in the Manafwa bridge.

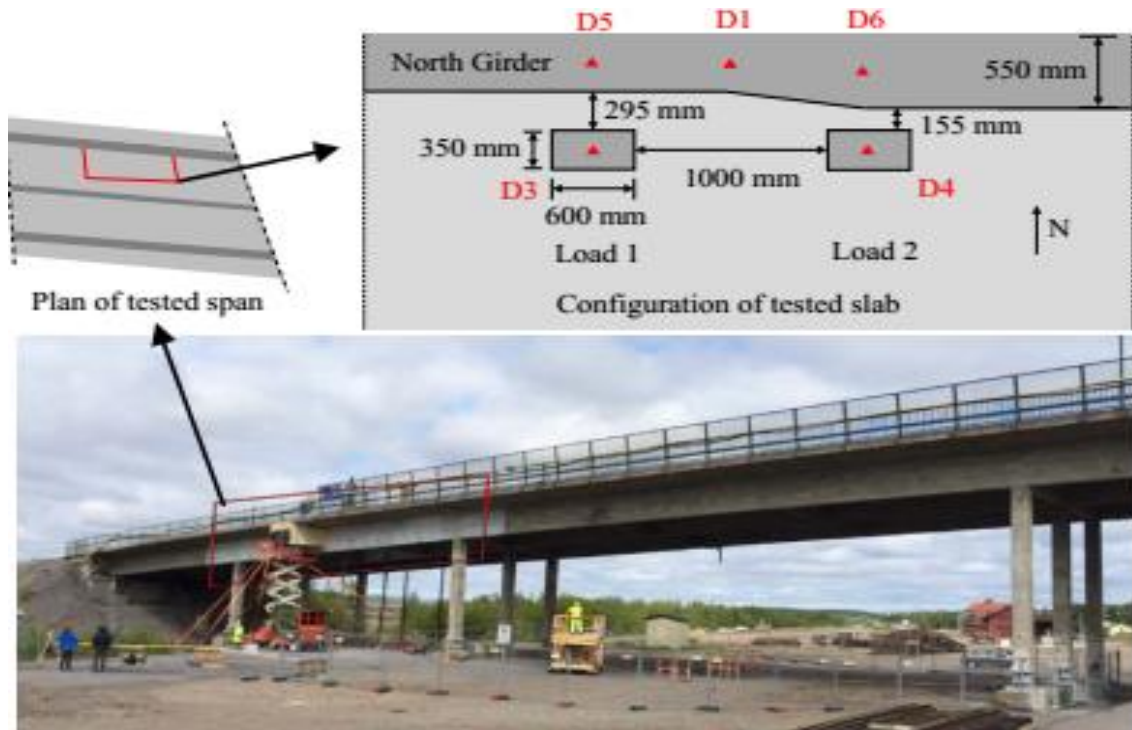


Figure 2-15 Geometry of the tested bridge (Shu, 2014).



Figure 2-16 Failed bridge deck slab after shear failure

CHAPTER 3. RESEARCH METHODOLOGY

3.1 INTRODUCTION

The research was executed through a series of methods which included reviewing of the available bridge information, carrying out of sites visits and using simple analysis. The Figure 3-1 below shows the methodology used and the phases undertaken in carrying out the research. In the initial stages, the bridge was assessed using the available data at the initial stage. A simple calculation was also performed to check the deviation from the expected comparisons. The results from the initial stage determined the extent of the numerical analysis and the experimental model.

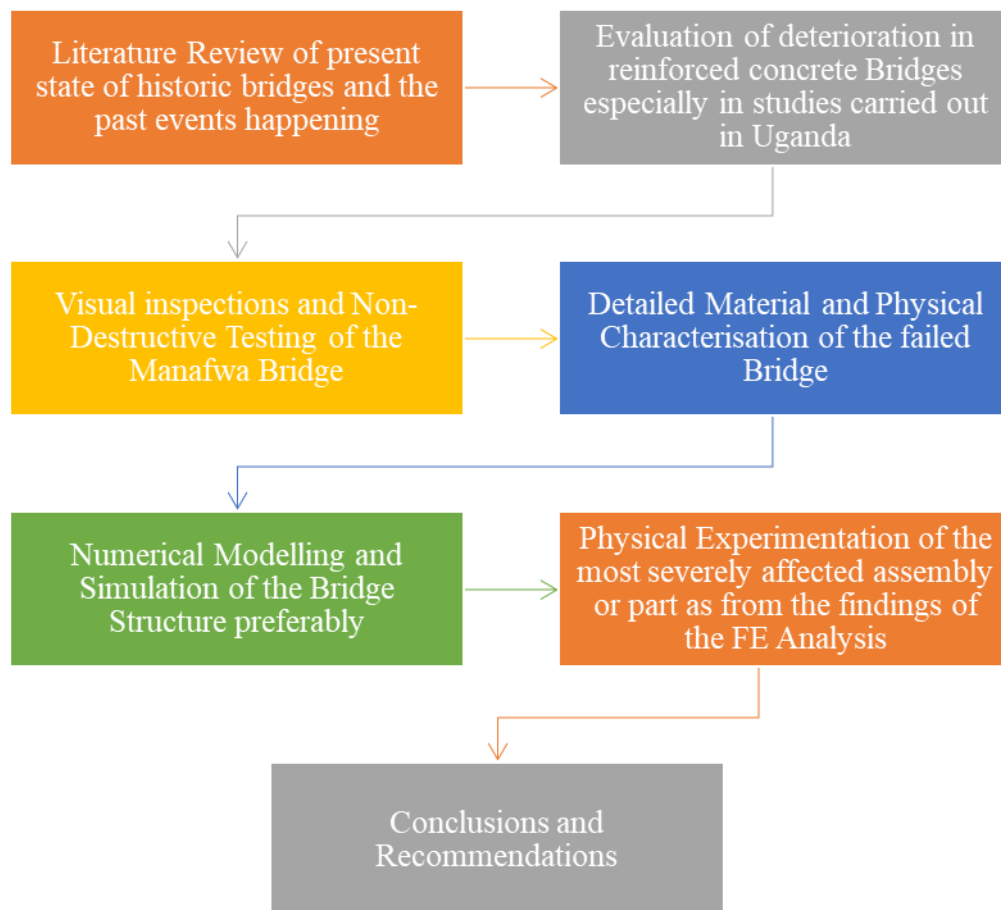


Figure 3-1 A detailed overview of the research process

3.2 STRUCTURAL CHARACTERIZATION OF THE FAILED HISTORIC BRIDGE

3.2.1 Desk study and site reconnaissance of the Manafwa Bridge

The desk study involved obtaining background information about the Manafwa Bridge which was then used as an input in the material characterisation and the structural assessment of the bridge. The desk study as such was conducted by visiting Uganda National Roads Authority which has the jurisdiction over all bridges found on the national road network, including the Manafwa bridge located on the national road Tororo – Mbale Road. Inquiries were made on the availability of information related to the

Manafwa bridge such as structural designs, inspection reports, design reviews and others. Unfortunately, because UNRA was only formulated in 2006, not much data was available with regards to this bridge and other historic bridges. Design protocols used by UNRA were given to me to enable comprehensive analysis in line with the standards and specifications of the country

3.2.2 Condition Assessment Survey

The conditional assessment survey of the Manafwa Bridge was carried out in accordance with Overseas Road Note 7 Vol 1 – A guide to Bridge inspection and data systems for District Engineers. The data was obtained using a template form in Bridge Inspection Report Form which is attached (one page of the filled form) in Appendix L. The Manafwa bridge was closed to traffic as a diversion bridge had been constructed to enable construction works of a replacement bridge to take place hence making the process of carrying out the study easy and unhindered. The steps undertaken in carrying out the conditional survey of the reinforced concrete bridge structure are looked at in the sections below;

Visual inspections were carried out on the bridge structure coinciding with the time period when the traffic counts were also carried out. The existing two-span bridge was assessed putting into consideration mainly the present condition of the bridge and the extent of damage that the bridge superstructure had incurred owing to the traffic flow on the bridge. The visual inspections were focused on:

- a) checking the overall safety and performance of the bridge structure.
- b) identification of any significant events leading to deterioration of the bridge such as major accident damage or other incidents or any other obvious failures of the components.
- c) Identification of potentially critical defects, for instance, cracks in deck slab etc.
- d) Photographic Records were taken of the bridge in the study capturing all the essential components of the bridge.

3.2.3 Non – Destructive Testing using Rebound Hammer

The primary purpose of the non-destructive testing carried out in this research project was to assess the properties of concrete limited to in-situ strength properties position, the condition of the steel reinforcement, concrete cover over the reinforcement and detection of defects of concrete members and the extent of visible cracks. Due to limitations in terms of financial resources and lack of equipment available, the research did not determine the durability, moisture content, extent of corrosion, presence of deleterious matter and chemical composition of the bridge.

The Rebound hammer method was the main method employed and was conducted as indicated below: following methods were used:

- The surface of the concrete was cleaned ensuring that it was smooth, clean and dry. The loose material was ground off and rough areas from poor compaction, grout loss, spalling or tooling were avoided as much as possible.

- To prepare the instrument for the test, the plunger was released from its locked position by pushing the plunger against the concrete.
- The plunger was then held perpendicular to the concrete surface and slowly pushed towards the test surface (Deck slab, parapet wall, abutment, piers and the footing).
- The test was conducted horizontally, vertically upward and downward and at varying intermediate angles depending on the accessibility of the surface.
- Results were then recorded. The plate 3-1 below shows the procedure explained above being undertaken on the bridge.



Plate 3-1 Schmidt Rebound Hammer used for the in-situ testing of the compressive strength

Correlation procedure of the rebound hammer used:

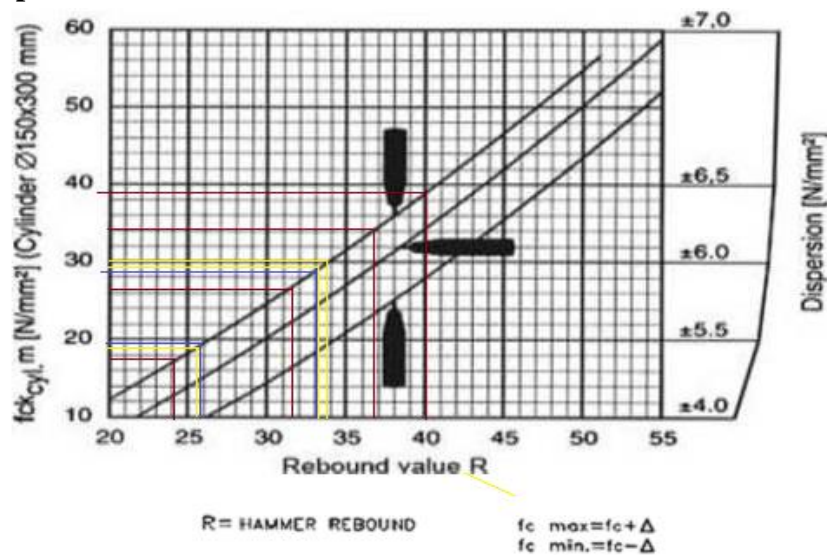


Figure 3-2 Conversion curve for the average compressive strength measured on cylinders.

Each rebound hammer is provided with correlation curves developed by the manufacturer using standard cube specimens attached in Figure 3-2 above. The values of compressive strength were therefore obtained by reading off the respective $f_{ck_{cyl}}$ on the given chart.

3.2.4 Destructive Testing using Coring

In order to carry out structural investigations and to verify and validate the compressive strength results of the Schmidt Rebound Hammer using a more direct strength assessment, core sampling and testing were carried out. The cores were extracted by use of a core drilling machine that makes use of a diamond-tipped core cutter cooled with water. The procedure entailed the following

- a) **Diameter of concrete core:** The cores obtained were of a diameter of 150mm, and on measurement in the lab were confirmed to be 145mm, which was in conformity to the specifications that require the diameter of the core specimen for the determination of compressive strength in load bearing structural members such as the deck slab to be 100 mm or 150 mm diameter; the preferred diameter size is 150 mm.
- b) **Length of concrete core:** Three core samples were successfully extracted with respective lengths of 172, 160 and 100mm. the first two cores fit within the requirement of length/diameter ratio for strength testing lying between 1 and 2. The third core, however, failed the length criteria. Consequently, a correction factor described in table 3-1 in accordance to ASTM C 42-77 was applied to the 100mm length core.
- c) **Core sampling methodology used:** Cylindrical core specimens were obtained from the drilling process with the ends being uneven. Because of the hole in the deck, there was reinforcement bars in the bottom of the layer as such the drilling was done in such a way that the core machine didn't encounter the reinforcements to avoid malfunctioning of the machine.
- d) **Moisture conditioning of concrete core:** After cores were drilled, surface drilled water was wiped off the and the surface moisture was allowed to evaporate. When surface appeared dry, they were placed in separate bags and sealed to prevent moisture loss. They were then maintained at ambient temperatures and protected from exposure to direct sunlight for at least 5 days after last being wetted and before testing.
- e) **Measurement and testing of the concrete core:** The core specimens were tested within 7 days after coring, and the compressive strength calculated using the computed cross-sectional area based on the average diameter of the specimen. For all cases where the L/D ratio was 1.75 or less, the results obtained were corrected by multiplying with correction factors as given below in Table 3-1:

Table 3-1 Correction factor for length to diameter ratios less than 1.75

L/D Ratio	Correction Factor
1.75	0.98
1.5	0.96

1.25	0.93
1.0	0.87

The pictures of the core sampling and cores obtained are attached in Plate 3-2 below:



Plate 3-2 Core Testing being done on the deck's slab

3.2.5 Structural Steel Reinforcement –Tensile Strength Tests

During the coring process, a number of steel reinforcement bars exposed by the open hole were cut and taken to the laboratory in addition to the concrete cores. The steel was cut in such a way to have appropriate depth for the test to be carried out. The samples were used in the laboratory to determine the following:

- a. The size (diameter) of the steel rebars used in the deck slab using Vernier Callipers
- b. The ultimate tensile strength of the two main types of reinforcement using the materials testing machine at the Makerere University mechanical laboratory
- c. The chemical composition of the steel reinforcement bars to determine the extent of carbonation, and other chemical properties pertinent in investigating the failure mechanism of the deck slab.

3.3 NUMERICAL ANALYSIS OF THE HISTORIC BRIDGE

3.3.1 Introduction

During the Numerical simulation, the bridge structure was analysed as a composite structure, as the girders were clearly made of steel while the deck is concrete. The software used for the carrying out the simulations of the bridge was ANSYS 16.0 which

was procured with a one-year operational license for strictly studying purposes only. The information (FEM input data used for the simulations was all obtained from the previous section of structural characterisation of the historic bridge. Because of the lack of sufficient information including the design calculations and drawings, some parameters required for the analysis were not available for the study, consequently, the design parameters as per the Uganda Roads and Bridges Design Manual 2010 were used in the software.

3.3.2 FEM Input Data

For the reinforced concrete bridge structure, Finite Element Software called ANSYS was used and required the input of data for material properties obtained in the previous section as follows: Elastic modulus (E_c), Ultimate uniaxial compressive strength (f'_c), Ultimate uniaxial tensile strength (modulus of rupture, f_r), Poisson's ratio (ν), Shear transfer coefficient (β_t) and Compressive uniaxial stress-strain relationship for concrete.

3.3.3 Bridge Loads determination - Traffic inventory and assessment

The deterioration of bridges and highway roads is primarily caused by the traffic using the structure is mainly due to the magnitude of the individual wheel loads and the repetitions or the number of loads that are applied over time. The Uganda Ministry of Works and Transport (MoWT) road design manual 2010 stipulated 7-day classified traffic counts carried out along the diversion bridge for the case of the Manafwa Bridge as the same traffic that was using the failed Bridge is the same traffic using the new diversion. However, for the study, traffic counts were carried out for four days. The traffic data was however extrapolated as indicated in Appendix I and J to reflect the entire 7 days, this is provided for in the MoWT (2010). Additionally, the analysis concentrated on the peak hours and were carried out for both night and daytime. The data was analyzed as shown in Appendix H to obtain the equivalent standard axle load of 994 ESALs.

3.3.4 ANSYS Modelling

The project schematic that was followed in executing of the simulation in ANSYS is shown in the Plate 3-3 below. The type of analysis used was the static structural analysis. Engineering data indicated in the section 3.3.1 above and obtained from the structural characterisation study was input into the software. The geometry which was created in Solid Works was then imported into the software and the thicknesses of the elements input.

A	
1	Static Structural
2	Engineering Data ✓
3	Geometry ✓
4	Model ✓
5	Setup ✓
6	Solution ✓
7	Results ✓

Plate 3-3 Project Schematic indicating completion of the analysis

The imported geometry shown in Figure 3-3 below was then converted into the required model by assigning material properties to all the constituent bodies of the geometry. After the model parameters were defined, the modelling was set up by carrying out the meshing of the elements, providing the boundary conditions and assigning the different loading conditions. The software was then requested to evaluate the solution to provide the simulation. The software generates a detailed solution report of which some of the information is provided in Appendix D.

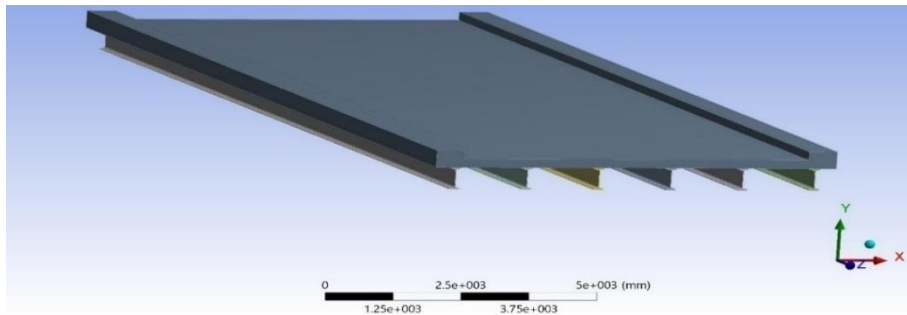


Figure 3-3 Full bridge model as applied in the ANSYS program (Isometric 3-D view)

Three different models were analysed to represent the full bridge failure shown in Figure 3-3 above, the probable failure in one span of the bridge (also referred to as the half-bridge model) and the third was to depict the localized failure of the deck slab in between the two I-girder supports which is referred to as the failed deck slab model in Figure 3-4 below.

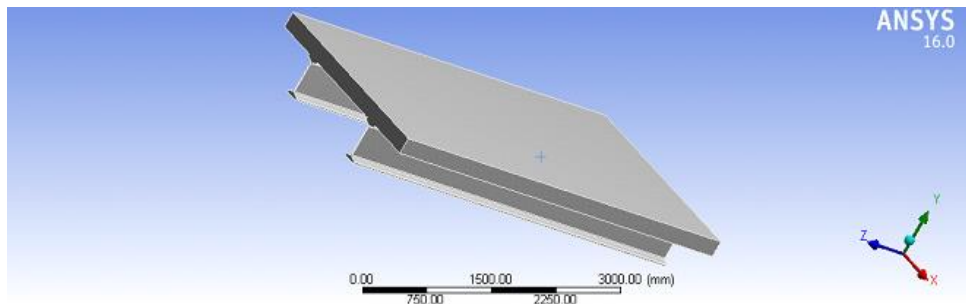


Figure 3-4 Failed Deck slab Model

After inputting all the requisite primary data as described above, the solution is run as shown in Figure 3-5 below taken while executing the numerical analysis.

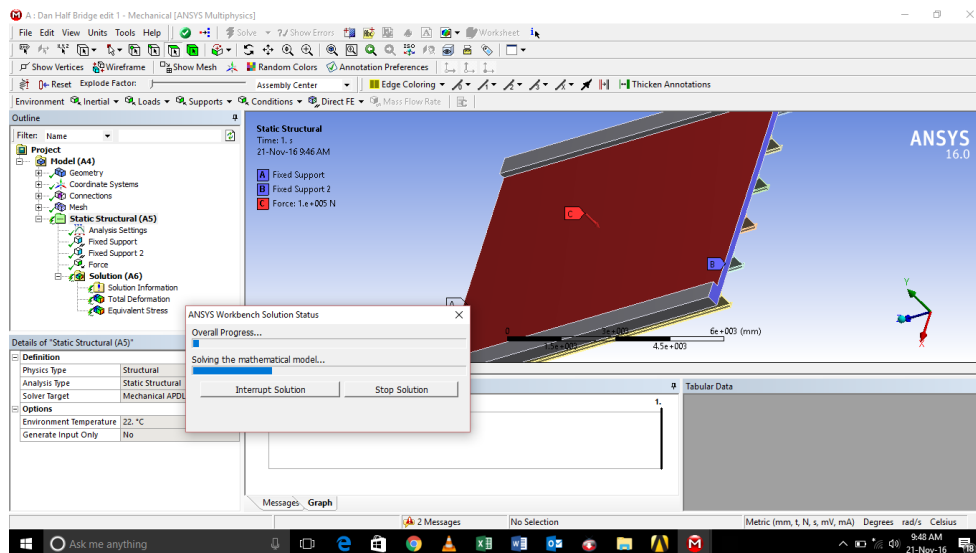


Figure 3-5 Processing of the Mathematical ANSYS solution ongoing

3.4 EXPERIMENTAL MODELLING OF THE BRIDGE DECK SLAB

The deck slab of the Bridge spans 20m with a width of 7.8m. The failure of the section was predominantly by punching with a hole developed between two girder supports. Given the laboratory restrictions that could not allow the testing of the entire bridge deck slab the modelling of the deck slab focused on the deck slab between the two girder supports. The process followed in the determination of the size of the experimental model included the following:

3.4.1 Definition of the scope of the problem/experimental testing

The scope of the experimentation was to carry out a concentrated or point loading (load applied at the centre of the slab) test on a deck slab element depicting the entire deck slab lying between two girder supports.

3.4.2 Specifying of similitude requirements for geometry, materials and loading

The actual slab had a fixed support at the abutment ends, while over the girder supports it was freely supported. As such this was depicted in the laboratory by casting a slab with a width slightly more than the required distance between the girder supports to allow for over-lapping to enable the slab to be able to support the continuous effects such as bending moment. The actual geometry of the bridge was big to be applied in the laboratory as such a geometric scale factor of 2 was used. Implying the dimensions of the actual deck slab was reduced by 2 in the fabrication of the model deck slab for experimentation in the laboratory.

3.4.3 Sizing of the physical model

From the similitude requirements for the geometry, a scale factor of 2 was used. As a result, dimensions of the model were determined by the reduction of the dimensions in the prototype by 2 using the equation no. 1 below. The space between two girders in the prototype bridge is 1400mm which is reduced to 700mm in the model and the thickness

of the deck slab is 200mm which is reduced to 100mm. A length of 1000mm was used, as the main determinant of failure for the deck slab anticipated in this experiment is punching shear failure and bending moment as such no limitation in length as shown in the Plate 3-4



Plate 3-4 Experimental model scaled down using a geometric scale of 2

The scaling down of the prototype also included the scaling down of the area of the reinforcement bars from R16 and R12mm with a reduced diameter and the spacing. Consequently, the length of the deck slab cast was 1000mm and the width was 700mm as shown in Plate 3-2 above of the experimental setup.

$$\text{Scale Factor} = \frac{\text{Length in prototype (Actual Bridge)}}{\text{Length in experimental model}} \quad \dots\dots\dots \text{Equation 1}$$

3.4.4 Selection of Model Materials

The principle of the physical experimentation was to compare the current state of the bridge as at failure to the design parameters. The exact design of the Manafwa Bridge was not obtained, however, the Uganda Bridge Design Manual, the stipulated minimum concrete compressive strength of all similar bridges and from the current ongoing bridge projects is 30 MPa. The in-situ concrete strength obtained by the tests carried out in the above sections was compared to the baseline concrete strength of 30MPa which was also used to cater for the deterioration of concrete with age. Consequently, two deck slabs were cast in the laboratory, one of compressive strength of 12.9MPa to depict the actual site conditions and in-situ strength, and the second slab of 28MPa obtained to depict the design strength. The mix design was carried out using the DoE method and the sample form used is attached in Appendix K.

3.4.5 Fabrication phase of the Deck Slabs

The first step in the fabrication phase was to make the formwork to the right internal dimensions to enable casting of a deck slab with the desired parameters. The formwork is shown in the Plate 3-5 below. After the setting up of the formwork, the steel reinforcement bars were cut into short pieces 5 pieces of R6 bars and 11 pieces of R8 of 950mm and 650mm length respectively. The casting of concrete then ensued after thorough examination using visual inspections of the set-up to ensure that the

reinforcement spacing was as specified and that the steel rebars were not rusty. At casting, the concrete cubes were cast for checking of the concrete strength of the cast slabs.



Plate 3-5 Fabrication process of the Deck Slab model in the laboratory

3.4.6 Instrumentation and recording equipment for displacements and forces

The deck slab was tested in a loading frame and rested on simple supports (rectangular steel sections of width 100mm which closely depicts the required width 95.25). To align the deck slab vertically and prevent lateral distortions, horizontal simpler supports were provided on either side. The aligning vertical steel frame was clamped onto the main steel frame. To enable the loading of points on the top chord members by hydraulic jacks attached to the loading frame, vertically positioned steel sections extended from the relevant joints of the beam up to the appropriate level underneath the loading jacks. Load cells were then positioned directly over the centre of the slab using sufficient steel spacers to distribute the applied load.

3.4.7 Loading Systems and Conditions

A static experiment was used during the loading with a point/concentrated loading applied. The testing was carried out by gradually applying loads using a loading cell which load magnitude was increased gradually using the loading cell until the point of failure.



Plate 3-6 Transducer being configured prior to testing and Loading using a Load cell.

Load application was by means of hydraulic jacks as shown in plate 3-6 at the top point connected exactly at the centre of the slab. The loads were applied gradually and their magnitudes measured by load cells connected to an electronic data logger or strain meter. Deflections were measured by LVDTs linked to the data logger while strains were measured by the attached strain gauges, also linked to the data logger.



Plate 3-7 Strain gauges connected to the transducer and the LVDT connected to the Loading Cell to measure deflection at the centre of the slab.

CHAPTER 4. RESULTS, DISCUSSION AND ANALYSIS

The results are classified as per the specific objectives of the research thesis and in order of the research, methodology used. The analysis and discussion is also included after discussion of the actual results obtained in the study.

4.1 STRUCTURAL CHARACTERIZATION OF THE FAILED HISTORIC BRIDGE

4.1.1 Conditional Assessment Survey of the Bridge

The Manafwa bridge is a composite deck bridge as in described in section 2.1 of the literature review. The visual inspections were carried out that showed that the superstructure deck slab system had developed a relatively large hole between the two longitudinal steel beams located adjacent to the carriageway centreline on the left lane (Tororo – Mbale Direction) on the first span from the Tororo side. In summary, the observations below were recorded from the condition survey and visual inspections:

- i). An examination of the opening in the bridge superstructure slab revealed that there is no hogging reinforcement in the slab, the concrete looks weak and that the longitudinal steel beams appear to have no shear connectors.
- ii). The maximum length of the opening that is parallel to the traffic flow direction was obtained as 2530mm and 1350mm in the direction normal to the traffic flow stream.
- iii). Cracking was observed in the deck slab that was noticeable at a similar position on the second span as in the first span from Tororo with the hole.
- iv). The abutments and pier are in good visual condition and have structural integrity as they are still intact visually as can be seen in the Plate 4.1 below.
- v). The by-pass used is 18 km long gravel road with single lane bridge structure. The by-pass requires widening and more cover to pipe culverts to avoid damage by heavy trucks.

Detailed inspections were then conducted on the bridge using the Overseas Road Note No. 07 bridge inspection report and the following were noted:

- a) Two longitudinal beams were exposed for shear connector examination. The beams do not have shear connectors apart from diameter 12mm round mild steel L-shaped bars welded to top flanges and spaced more than 2.5m.
- b) A close examination of superstructure longitudinal steel beams revealed that they are all discontinuous over the pier.
- c) There was scouring on the upstream side of the pier footing to a depth of about 260mm below footing soffit. The footing concrete vertical faces protrude beyond the mass concrete vertical faces by 150mm at upstream and at downstream faces and by 400mm at faces parallel to abutments.
- d) The superstructure slab is plastered on the underside to conceal exposed reinforcement but the plaster is falling off.
- e) Large isolated areas on the underside of the superstructure slab show deep

honeycombing. A lot of fines were lost during concreting of the slab thus the slab has a porous structure hence the brittle failure mechanism exhibited at the opened section.

- f) Part of surfacing and concrete along a crack in superstructure over pier was removed to examine the extent of cracking and whether the deck was continuous over the pier. The cracking continues to the bottom of the slab and there is no hogging reinforcement. The two-span deck is not continuous over the pier. No proper joint was provided at construction stage.
- g) Dimensions of the pier footing, columns and column capping beam were recorded including steel beam spacings, depth and flange thicknesses and concrete slab thicknesses.



Plate 4-1 Bridge geometry as observed on site

4.1.2 Bridge Superstructure Geometry

The 20m long superstructure has a 200mm thick solid concrete slab cast on 6 steel I-section beams as shown in Figure 4-1 and Plate 4-2. Concrete parapet posts are cast monolithic with the slab and two galvanised circular hollow section handrails are provided between the posts. The figure below shows the bridge cross section. Expansion joints were not noticed on the bridge deck soffit. However transverse cracks were noticed at the three support positions in the surfacing.

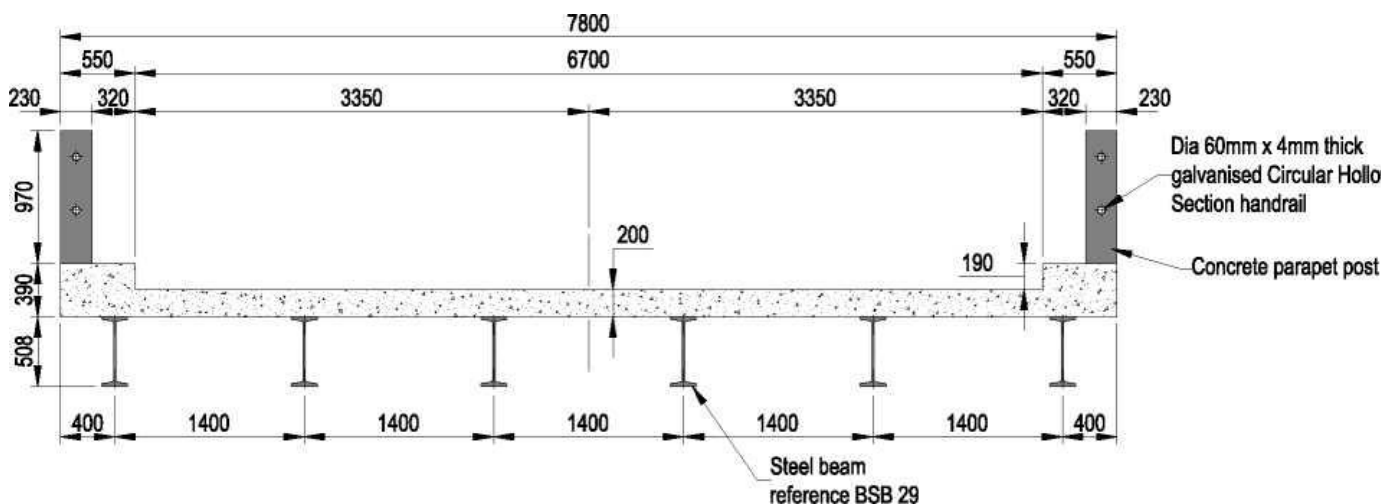


Figure 4-1 Manafwa River Bridge superstructure cross section



Plate 4-2 No hogging reinforcement in the slab, the concrete looks generally weak with a higher percentage of coarse materials

4.1.3 Steel I-Beam Section

The geometry of the typical cross-section of the I-girder beam including mainly the dimensions and cross-section measured during the detailed evaluation of the steel beams is as shown in the Figure 4-2 and Plate 4-3 below;

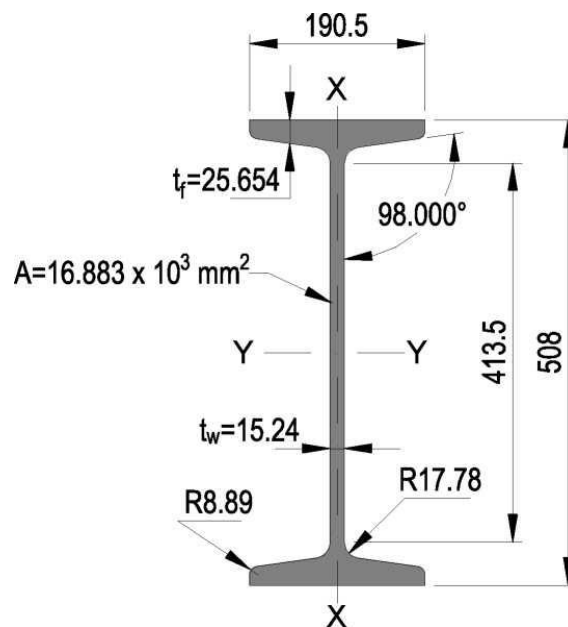


Figure 4-2 Steel beam cross section

The longitudinal steel beams are fixed in concrete at each abutment end. The six beams are continuous over the pier with a small non-uniform gap between the beam ends which could be a result of welding failure. The longitudinal steel beams have compression flanges fully restrained against rotation in the plan at abutment support and free to rotate in the plan at the pier support. It was also observed that the I-girders are continuously restrained by slab at compression flange level. Because of the discontinuity of some longitudinal beams over the pier, the deck is non-continuous. There is no information on the steel grade and quality for the longitudinal beams and a design strength of 250 N/mm² shall be used for all steel beam elements.



Plate 4-3 Bridge underside showing steel beams and pier.

4.1.4 Visual Inspection photography

The Plates 4-4 to 4-6 below show the state of the bridge superstructure at the time of inspections.



Plate 4-4 Manafwa River Bridge superstructure cross section immediately after the failure.



Plate 4-5 Transverse cracks in deck surfacing and concrete patching.



Plate 4-6 Opening in superstructure slab showing longitudinal steel beam, bottom reinforcement, disintegrated concrete layer and gravel layer under surfacing.

4.1.5 Schmidt's Rebound Hammer Test Results

The chart below was used to convert the in-situ test results of the rebound number to the average compressive strength of different elements of the Manafwa bridge. As indicated in the methodology, there were rebound numbers less than 20, extrapolation was done in order to determine the compressive strength. The summary of the in-situ concrete strength test results from the Schmidt rebound hammer for the major elements is shown in the Figure 4-3 below and the detailed results are attached in Appendix A.

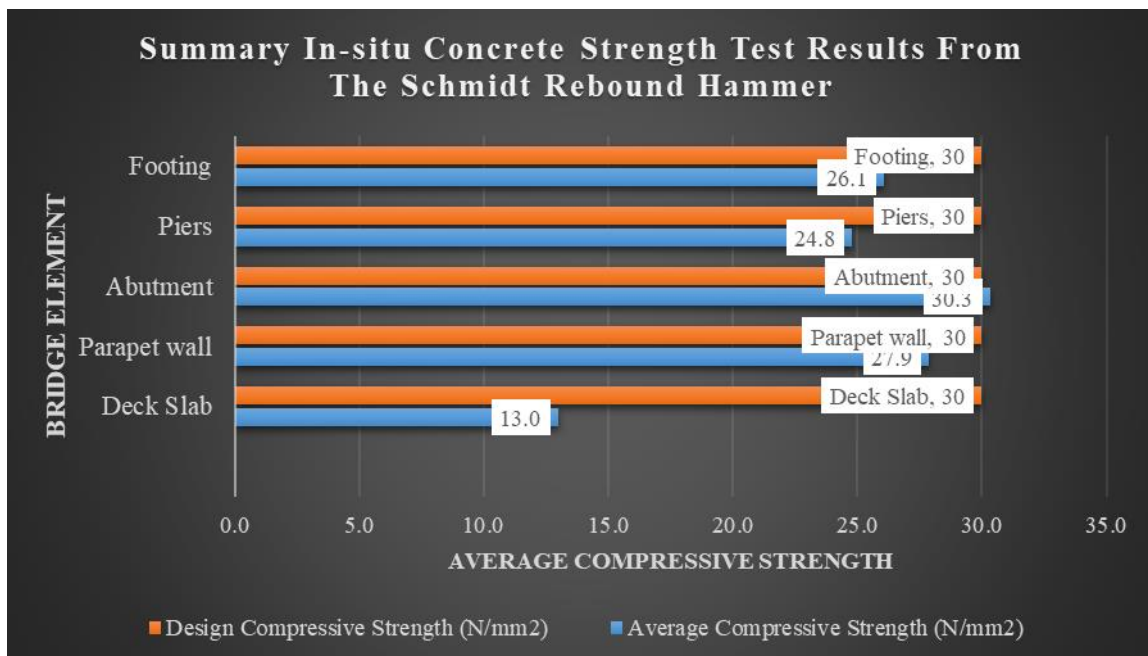


Figure 4-3 In-Situ Concrete Strength Test Results From The Schmidt Rebound Hammer

Discussion of results:

The values obtained show for the average compressive strength of the substructure of the bridge showed that the compressive strength of the piers, abutment and the footing was on average 28N/mm² which is close to the design compressive strength of 30N/mm². The

variation in the strength can be attributed to ageing and fatigue as the bridge has been in existence for over 80 years since construction. These results also indicate that the substructure did not suffer any form of failure and can be maintained for further use as it still has its structural integrity.

The compressive strength of the deck slab obtained from the rebound hammer test was, however, very low of 13N/mm^2 in comparison to the design concrete strength class. The concrete also exhibited a lot of coarse materials and was loose which was evidence to support the loss strength results. The results formed the basis for carrying out the destructive testing on the deck slab to further ascertain the low concrete strength and to provide an input to the numerical modelling undertaken.

4.1.6 Destructive Test Results - Core Test

The compressive strength values of the bridge deck obtained from the testing of the three core samples obtained from the field are summarised as in the Figure 4-4 below. The detailed results are attached in Appendix B.

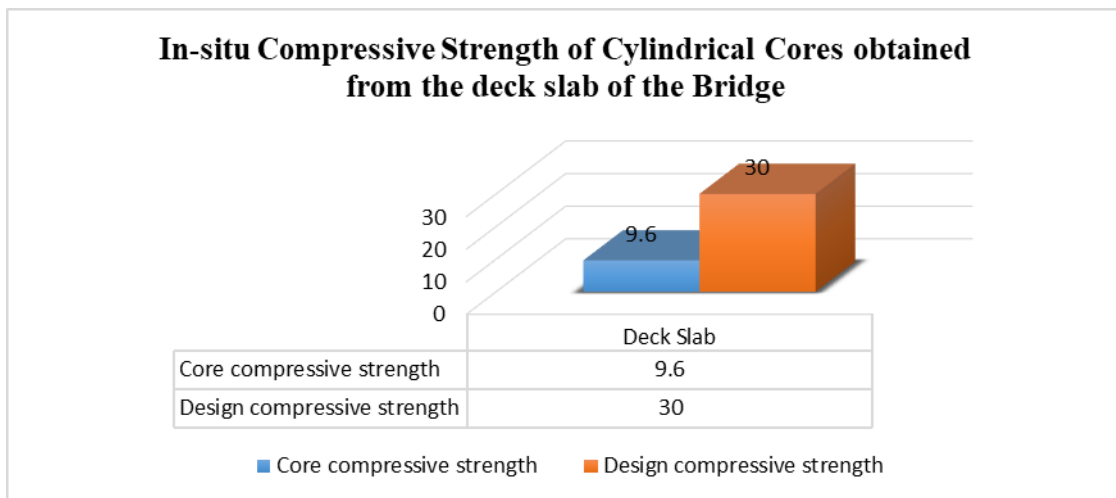


Figure 4-4 Summary of the core compressive strength results of the deck slab

Discussion of results

The compressive strengths of the three cores obtained from the deck slab are shown in figure 4-4 above. The mean compressive strength of the Deck Slab is very low (9.6N/mm^2) as shown in Figure 4-5 below. The results of the rebound hammer correspond with the core tests as both shown that the deck slab had a very low compressive strength. This is one of the reasons why the deck slab failed by punching shear. Because of this observation, the punching shear capacity was determined in the next section 4.2 to ascertain if the decreased concrete strength could not cope with the punching shear capacity of the deck slab.

In addition, it is possible that the concrete weakening at the point of failure could have been a result of the fatigue and corrosion behaviour described in section 2.2 of common causes of structural failure in bridges that could have weakened the concrete over time hence resulting into the failure of the Bridge. Therefore, the major failure can be

attributed to the significant deterioration of the concrete which as a result could not withstand the applied load on the bridge hence the collapse.

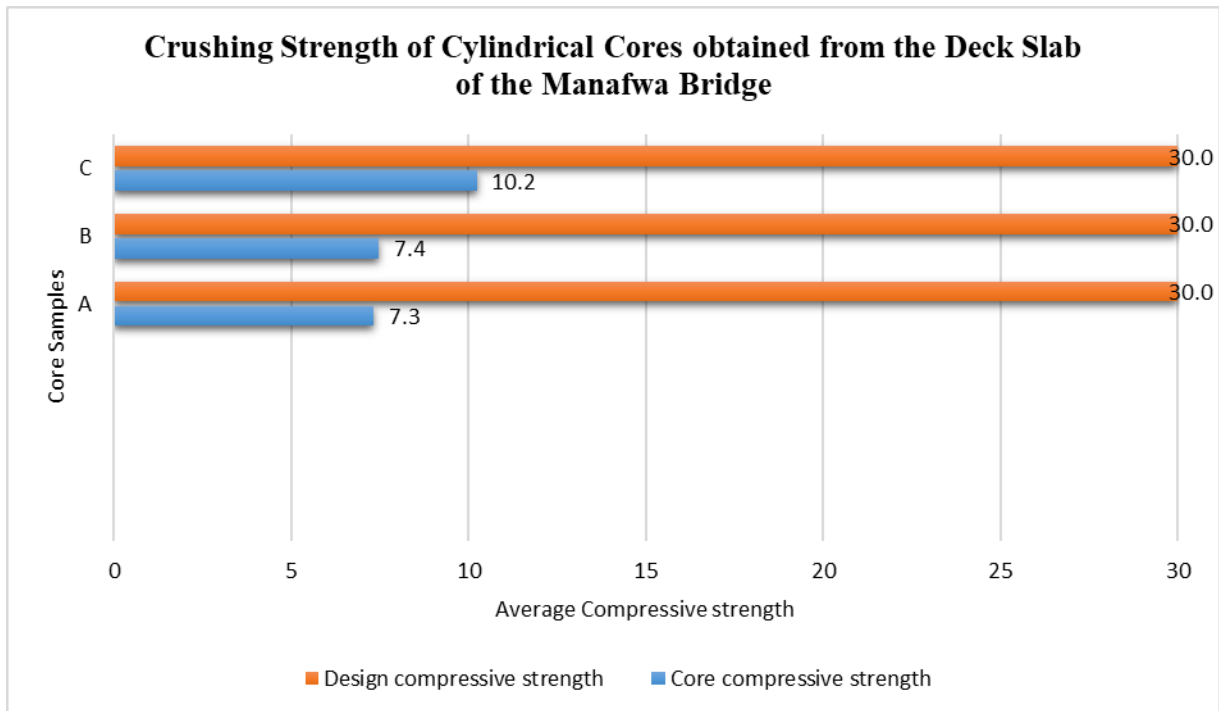


Figure 4-5 Field Crushing compressive strength of cylindrical cores obtained from the deck slab of the Manafwa Bridge

4.1.7 Structural Steel tensile strength Tests

The tests carried out on the reinforcement bars are indicated in the electronically generated graphs obtained from the Testometric Materials Testing Machines in the Makerere University Mechanical workshop attached in Appendix C. the findings showed that there are two sizes of reinforcements used in the deck slab: 12mm round bars each at an average spacing of 100mm in the transverse direction at the bottom of the layer and the main longitudinal reinforcement bars are 16mm round bars each at a spacing of 175mm centre to centre.

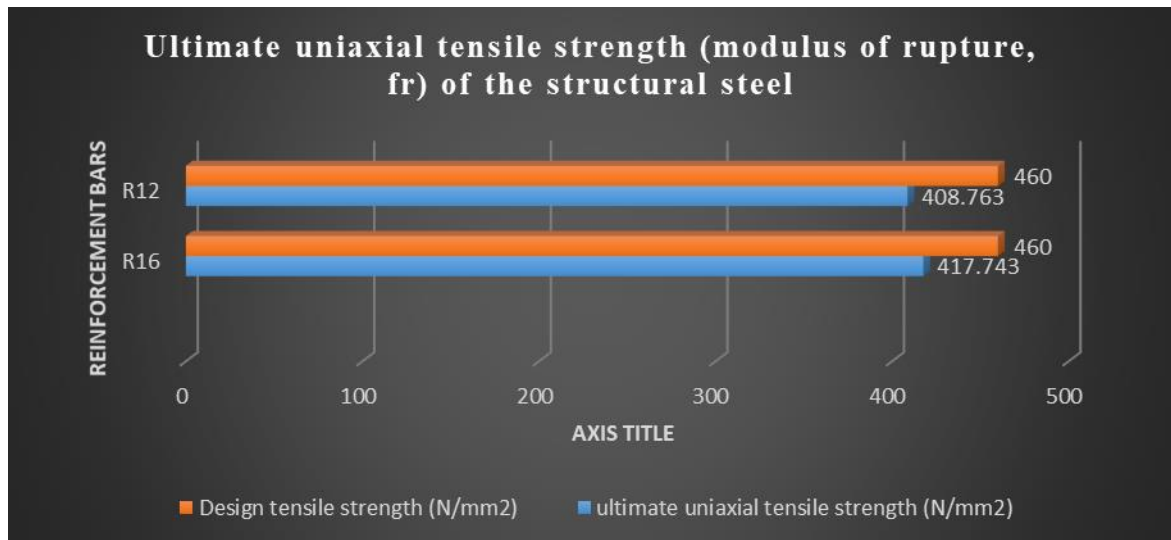


Figure 4-6 Tensile strength of the reinforcement bars

The tensile strength of the reinforcement bars at the peak also referred to as the ultimate uniaxial tensile strength (modulus of rupture, f_r) of the structural steel obtained was 408.763 N/mm² for the R12 bars and 417.743 N/mm² for the R16 bars shown in the Figure 4-6 below. The design strength for the reinforcement bars is 460 N/mm² which indicates that the rebars had a reduced tensile strength bearing capacity. This could be attributed to the ageing and fatigue over time. Additionally, the bars were exposed to air and water and had shown signs of corrosion which could have contributed to the reduction in tensile strength.

The lower tensile strength of the rebars could also be attributed to the ageing and fatigue over time. Additionally, the bars were exposed to air and water and had shown signs of corrosion which could have contributed to the reduction in tensile strength. The reinforcement bars were tested for chemical content and the results showed in Figure 4-7 were obtained indicating that the bars were prone to chemical attack with manganese the most common followed by carbon and chromium.

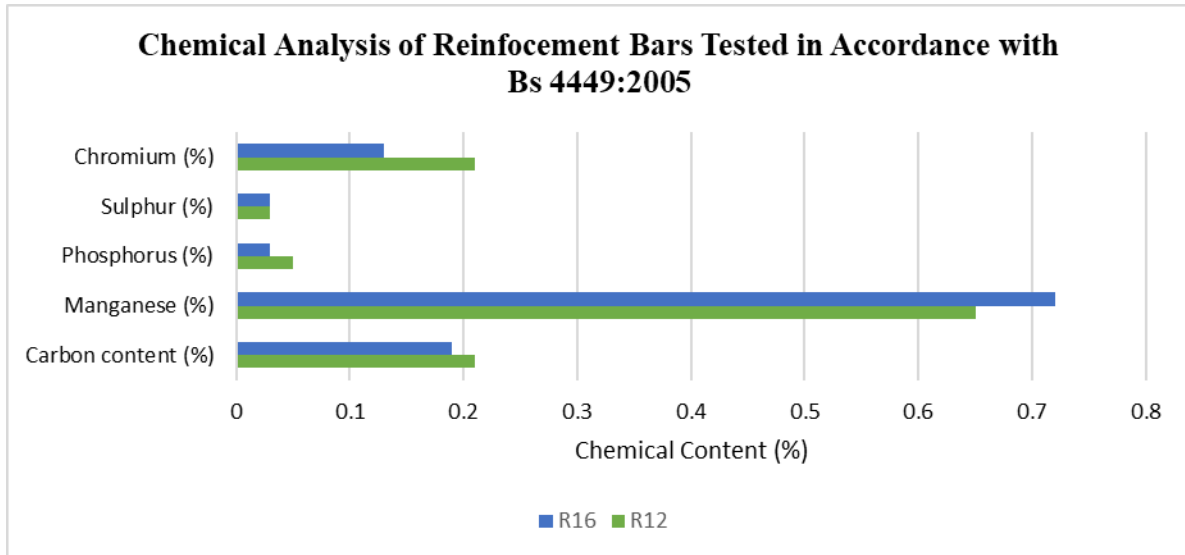


Figure 4-7 Chemical Analysis of Reinforcement Bars Tested in Accordance with BS 4449:2005

4.2 STRUCTURAL EVALUATION AND ASSESSMENT

4.2.1 Superstructure Slab Shear Capacity Under Concentrated Loads

Load at the middle of the slab: Reference is made to BS 5400, Part 4, 1990 Clause 5,4,4,2. Let the subscript L denote a direction parallel to the longitudinal direction of the slab (traffic flow direction from Tororo to Mbale) and direction perpendicular to it (transverse direction). The superstructure slab has bottom reinforcement of R16 at 100mm centres in the transverse direction at the bottom most level and R12 at 175mm centres in the longitudinal direction on top of R16 bars. There is no top slab reinforcement. The concrete cover to bottom most steel is 20mm and the slab thickness is 200mm.

$$\begin{aligned}
 d_t &= 200 - 20 - 16/2 &= 172\text{mm}, \\
 A_{t \text{ steel prov}} &= \text{R16 at 100} &= 2010\text{mm}^2/\text{m} \text{ and} \\
 d_L &= 200 - 20 - 16 - 12/2 &= 158\text{mm}, \\
 A_{L \text{ steel prov}} &= \text{R12 at 175} &= 665\text{mm}^2/\text{m}
 \end{aligned}$$

Further Reference is made to BS 5400, Part 2, 1978, Clause 6,3,2 as shown in the figure attached below, assume no dispersion of HA single wheel load to the surface of the slab. A square contact area 300mm x 300mm will be assumed at the middle of the slab. The critical perimeter of the deck slab is shown in the Figure 4-8 below:

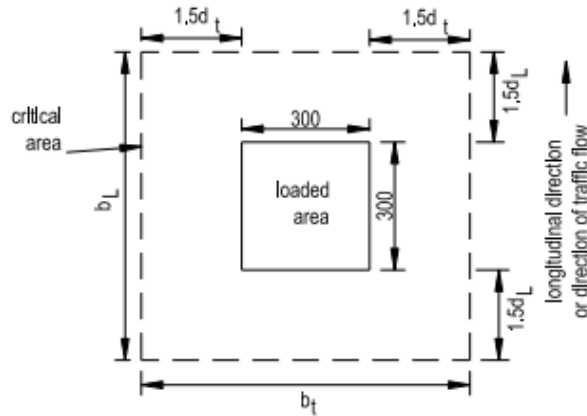


Figure 4-8 Shear Perimeter

$$b_t = 2 \times 1.5 \times 172 + 300 = 816\text{mm}$$

$$b_L = 2 \times 1.5 \times 158 + 300 = 774\text{mm}$$

Assuming HB37.5-wheel load was considered for design as observed for most bridges in Uganda, then the following will occur:

- The loaded area will be 291mm x 291mm (which is approximated to 300mm x 300mm in the analysis and in the shear perimeter drawing above).
- The ULS load will be 134.063 kN
- The closest spacing of HB wheels is 1000mm and
- The closest distance between the shear perimeters is $1000 - b_t = 193\text{mm} > 0$.

Therefore, the shear perimeters of adjacent HB37.5 wheels will not overlap.

The ULS load from the respective computations due to HA single wheel load is obtained as **165.000kN**. As such the ULS load due to HA single wheel load is greater than ULS due to HB37.5, that is to say, $165.000\text{kN} > 134.063\text{kN}$ for HB37.5. Use of HA single wheel load is critical for single loads.

In transverse direction: Reference is made to BS 5400, Part 4, 1990, Clause 5,3,3.

Ultimate Shear Stress:
$$v_c = \frac{0.27}{\gamma_m} \left(\frac{100A_s}{b_w d} \right)^{1/3} (f_{cu})^{1/3}$$

$$v_{cl} = \frac{0.27}{1.25} \times \left(\frac{100 \times 2010}{1000 \times 175} \right)^{1/3} \times f_{cu}^{1/3} = 0.228 f_{cu}^{1/3} \text{ N/mm}^2$$

$$\epsilon_{st} = \left(\frac{500}{175} \right)^{1/4} = 1.306 > 0.70$$

Take
$$\epsilon_{sl} = 1.306$$

As such,
$$\epsilon_{sl} v_{cl} = 1.306 \times 0.228 f_{cu}^{1/3} = 0.298 f_{cu}^{1/3} \text{ N/mm}^2$$

Hence

$$V_{cL} = \sum \varepsilon_{sl} V_{cl} b_t d_L = 2 \times 0.298 f_{cu}^{\frac{1}{3}} \times 774 \times 175 \times 10^{-3}$$

In longitudinal direction

Ultimate Shear Stress:
$$v_{cl} = \frac{0.27}{1.25} \times \left(\frac{100 \times 665}{1000 \times 158} \right)^{\frac{1}{3}} \times f_{cu}^{\frac{1}{3}} = 0.162 f_{cu}^{\frac{1}{3}} \text{ N/mm}^2$$

$$\varepsilon_{sl} = \left(\frac{500}{158} \right)^{\frac{1}{4}} = 1.334 > 0.70$$

Take
$$\varepsilon_{sl} = 1.334$$

As such,
$$\varepsilon_{sl} v_{cl} = 1.334 \times 0.162 f_{cu}^{\frac{1}{3}} = 0.216 f_{cu}^{\frac{1}{3}} \text{ N/mm}^2$$

Hence

$$V_{cL} = \sum \varepsilon_{sl} V_{cl} b_t d_L = 2 \times 0.216 f_{cu}^{\frac{1}{3}} \times 816 \times 158 \times 10^{-3}$$

$$V_{cL} = 55.697 f_{cu}^{\frac{1}{3}} \text{ kN}$$

Shear resistance at the critical slab section $V_c = V_{ct} + V_{cl} = 135.041 f_{cu}^{\frac{1}{3}} \text{ kN}$

Ultimate limit state shear load (ULS) exerted by the HA single wheel load is:

$$\text{ULS}_{\text{HA}} = 100 \text{ kN} \times 1.5 \times 1.1 = 165 \text{ kN}$$

ULS dead load of slab within the shear perimeter

$$\begin{aligned} \text{ULS}_{\text{Dead Load}} &= 0.816 \text{ m} \times 0.774 \text{ m} \times 0.2 \text{ m} \times 25 \text{ kN/m}^3 \times 1.32 \\ &= 4.168 \text{ kN} \end{aligned}$$

ULS superimposed dead load due to the 100mm thick asphalt concrete surfacing

$$\begin{aligned} \text{ULS}_{\text{Asphalt surfacing}} &= 0.816 \text{ m} \times 0.774 \text{ m} \times 0.100 \text{ m} \times 25 \text{ kN/m}^3 \times 1.925 \\ &= 3.039 \text{ kN} \end{aligned}$$

The shear force acting on the critical slab section

$$\begin{aligned} \text{Shear force, } V &= 165 \text{ kN} + 4.168 \text{ kN} + 3.039 \text{ kN} \\ &= 172.207 \text{ kN} \end{aligned}$$

Maximum shear stress allowed in the slab, τ , is lesser of $0.75 \sqrt{f_{cu}}$ or 4.75 N/mm^2

Maximum Allowable Shear,

$$V_a = \tau (2b_t d_L + 2b_L d_t)$$

$$= 524.112 \tau \text{ kN} > V_c > V$$

The condition $V_a > V$ should be satisfied

And No shear reinforcement is required when $V_c > V$

Table 4-1 Punching shear capacity of existing superstructure slab for loading applied at the middle point of the slab.

Concrete strength, f_{cu} , (N/mm ²)	Maximum allowable shear, V_a , (kN)	Shear capacity, V_c , (kN)	Applied shear, V , (kN)	Comment
5	878.963	230.917	172.207	No reinforcement required
10	1243.041	290.937	172.207	No reinforcement required
15	1522.408	333.040	172.207	No reinforcement required
20	1757.925	366.558	172.207	No reinforcement required
25	1965.420	394.862	172.207	No reinforcement required
30	2153.010	419.604	172.207	No reinforcement required

The above results in Table 4-1 show that the existing slab is adequate in punching shear for the different range of concrete strengths (including the current strength obtained from the non-destructive testing carried out) considered as such could not have failed due to punching shear.

Load at the edge of the slab: The carriageway portion of the superstructure slab is bounded by longitudinal beams and transverse abutment concrete wall into which the superstructure longitudinal beams are encased at ends hence there is no need to check for shear due to concentrated loads.

4.2.2 Superstructure Slab Moment Capacity

4.2.2.1 Moment capacity of the Existing slab

For a given amount of tension steel, A_s , of design characteristic strength, f_y , and effective depth, d , the ultimate limit state, ULS, moment capacity of a reinforced rectangular concrete section with no compression reinforcement, is obtained from the formula below obtained from a typical Bridge design example (derived from BS 8110):

$$M_c = \frac{M_u}{0.694} \left\{ 1 - \left(1 - \sqrt{1 - \frac{d f_y A_s}{3.313 M_u}} \right)^2 \right\} \text{ Where } M_u = 0.156 f_{cu} b d^2$$

f_{cu} = characteristic strength of concrete and b = width of concrete section.

Let the subscript L denote a direction parallel to the longitudinal direction of the slab (traffic flow direction) and t a direction perpendicular to it (transverse direction) as described in the previous section. The superstructure slab has bottom reinforcement of R16 at 100mm centres in the transverse direction at bottom most level and R12 at 175mm centres in longitudinal direction on top of R16 bars. There is no top slab reinforcement. The concrete cover to bottom most steel is 20mm and the slab thickness is 200mm.

$$d_t = 200 - 20 - 16/2 = 172\text{mm},$$

$$A_{t \text{ steel prov}} = \text{R16 at 100} = 2010 \text{ mm}^2/\text{m}$$

and

$$d_L = 200 - 20 - 16 - 12/2 = 158\text{mm},$$

$$A_{L \text{ steel prov}} = \text{R12 at 175} = 665\text{mm}^2/\text{m}$$

$$f_y = 250 \text{ N/mm}^2$$

The Table 4.2 below summarises the moment capacity of superstructure slab as obtained using the moment capacity formula above.

Table 4-2 Ultimate Limit State Sagging moment capacity of the Existing slab

Concrete strength, f_{cu} , (N/mm ²)	Moment Capacity in the transverse direction, M_{ct} , (kNm/m)	Moment Capacity in the longitudinal direction, M_{cL} , (kNm/m)
5	32.683	18.197
7.5	43.308	19.360
10	53.933	20.523
15	61.016	21.298
20	64.557	21.686
25	66.682	21.919
30	68.099	22.074

4.2.2.2 Superstructure slab applied moments

The applied moments are obtained using the equations in Table 4-3 below which is extracted from BS 6110 part 2 1997 cl. 3.5.2.4 Table 13.2 for the ultimate bending moments and shear forces.

Table 4-3 — Ultimate bending moment and shear forces in one-way spanning slabs

	End support/slab connection				At first interior support	Middle interior spans	Interior supports
	Simple		Continuous				
	At outer support	Near middle of end span	At outer support	Near middle of end span			
Moment	0	0.086FI	-0.04FI	0.075FI	- 0.086F	0.063FI	-0.063FI
Shear	0.4F		0.46F		0.6F		0.5F

**NOTE: F is the total design ultimate load ($1.4G_k + 1.6 Q_k$);
 l is the effective span.**

Source BS 8110 pt2 1997 cl 3.5.2.4 Table 3.12

The applied moments are therefore summarised in Table 4-4 below

Table 4-4 Superstructure slab applied moments

Load	Transverse moments	Longitudinal moments
------	--------------------	----------------------

	(kNm/m)		(kNm/m)	
	Sagging	Hogging	Sagging	Hogging
Permanent	1.4	2.2	0.9	0.4
Permanent and HA single wheel load	4.0	36.0	19.3	9.6
Permanent and HA	10.2	6.8	5.3	0.8
Permanent, HA and HB20	20.3	22.2	11.3	8.0
Permanent, HA and HB25	20.2	22.1	13.8	9.7
Permanent, HA and HB37.5	24.9	21.8	19.9	13.7

4.2.2.3 Summary and Analysis of the Results

The applied transverse sagging moments are all less than the slab moment capacities for the concrete strengths considered. The applied longitudinal sagging moments are all less than the slab moment capacities for the concrete strengths considered except for 5 MPa and 7.5 MPa concrete. This implies that there was a significant deterioration of the concrete which as a result could not withstand the applied moments hence the collapse. No hogging reinforcement was provided in the existing slab.

4.3 EXPERIMENTAL MODEL - LABORATORY RESULTS OBTAINED

4.3.1 Concrete Mix Design for the 30MPa and 13MPa Deck Slabs

Sieve analysis was done for sand to examine the grading of particles. The Sieve analysis test was used to provide the distribution pattern of aggregates sizes. The fineness modulus and the passing percentage of sieve No. 600.0 μm were obtained from sieve analysis test. These two factors were used in the mix design of the concrete mixes. River sand was used in this research. Before testing, the sand material was sieved using the sieve No. 10.0mm to ascertain that there weren't any particles with sizes more than 10.0mm. The Figure 4-9 below indicates the results obtained from the sieve analysis test of the sand. The Fineness modulus of the sand was calculated as described by (Neville, 1981). It was obtained from sieve analysis test as described in Table 9. Furthermore, the passing percentage of sieve No. 600 μm was 45.3%.

$$\text{Fineness Modulus (F.M.)} = \frac{\text{sum. of cumulative weight retained}}{100}$$

$$F.M. = \frac{0.1 + 2.5 + 7 + 12.4 + 26.9 + 54.7 + 86.1 + 97.9}{100} = 2.88 \%$$

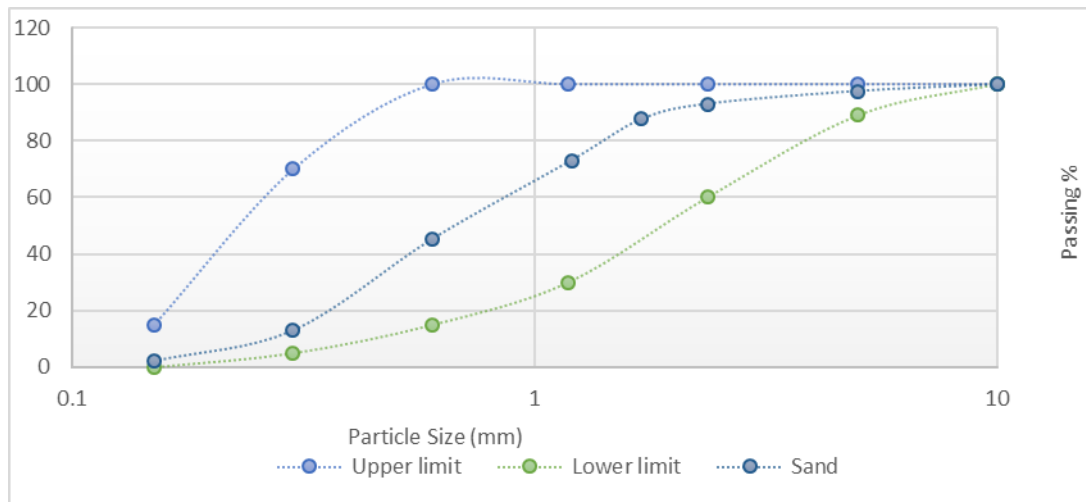


Figure 4-9 Sieve analysis result of the sand

BS 882:1992 specified requirements which were represented in limits. Grading curve of the sand should be between the upper and lower limits. Hence, the results indicate that the concrete used has the desired qualities. The coarse aggregates used also referred to as gravel were sieved, and the results illustrated in Fig. 4.10. A sample of 1000g weight was washed before testing. Thus, clay and any other materials were removed. The size distribution of the gravel was acceptable as Fig 4.2 shows. at sieve No. 20mm, the gravel gave 68.8 passing percentage, while the upper limit at that point was 70%. However, the gravel curve was placed between the required limits.

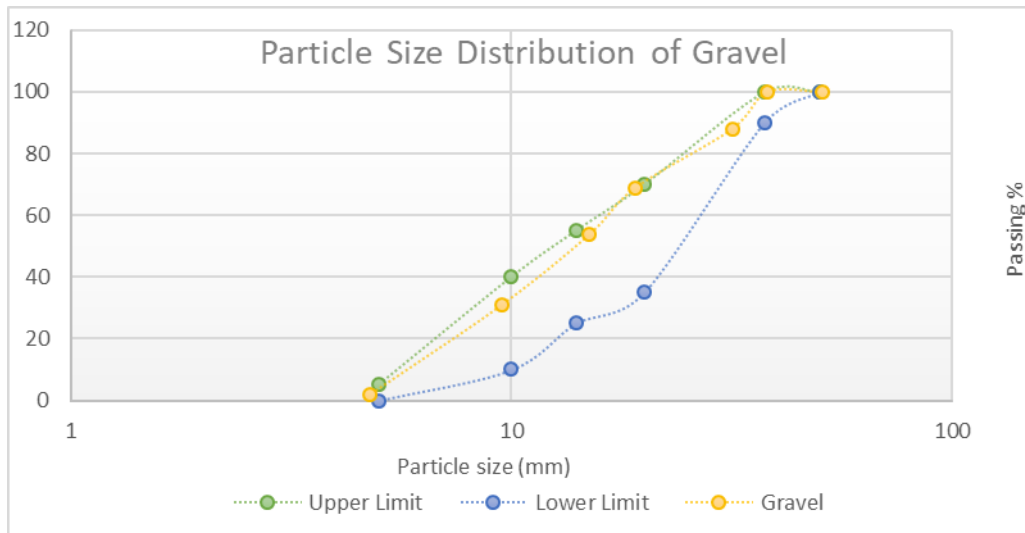


Figure 4-10 Sieve analysis result of the gravel

4.3.2 28MPa Deck Slab (depicting the Design bridge condition):

The deck slab failed as a result of cracks that progressively increased longitudinally with maximum deflection observed at the center of the slab. Signs of punching shear were evident as shown in the experimental set up in the Plate 4-7 below. The failure depicts the expected failure if the deck slab properties were in conformity to the design conditions.



Plate 4-7 Progressive failure of the deck slab with longitudinal cracks increasing in size till failure.

The Figure 4-11 below shows that the higher the loading the more the deflections as would be expected. The first crack in the slab was observed at a load applied equivalent to 107,047 N (equivalent to 10.91 tons) and was at a deflection of 31.35mm. At this point, the cracks were observed to run longitudinally in the deck slab. Further loading was applied and the graph clearly indicates that with a smaller loading interval, much deeper cracks and deformations were obtained as compared to the behaviour prior to the first crack where a smaller deflection was obtained with a bigger loading interval.

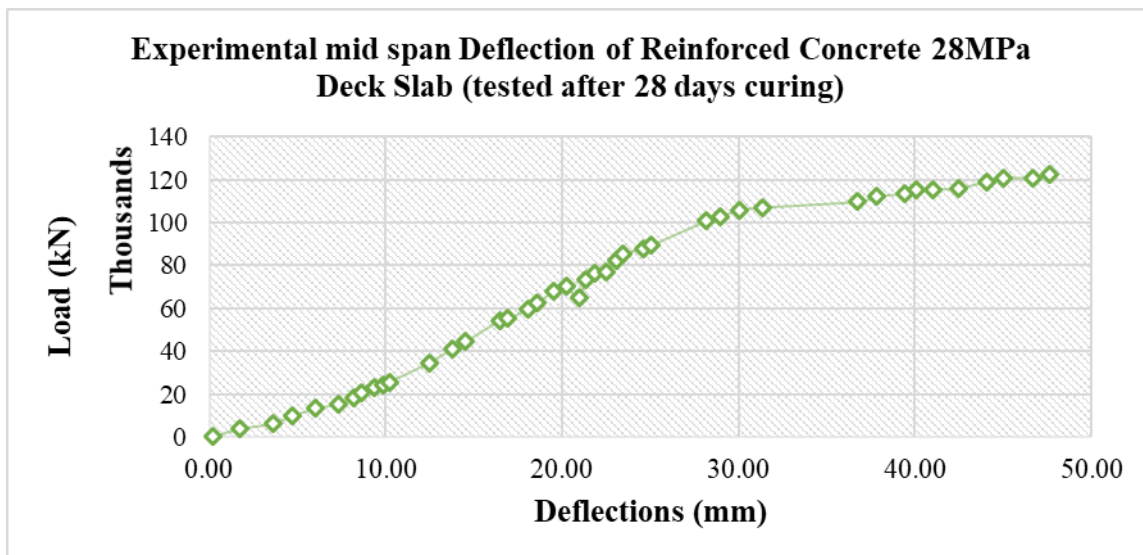


Figure 4-11 Graph for the Experimental mid-span deflection of the 28-day Deck Slab

Total failure of the deck slab occurred when a load of 122.272 kN was applied, and the total mid-span deflection of the 28MPa deck slab was 47.60mm. The length scale factor used in the modelling was 2. Using the above equation of Scale Factor, the deflection in the actual bridge is obtained as below:

$$Length_{\text{prototype}} = Length_{\text{exptal model}} \times \text{Scale Factor} = 47.60 \times 2 = 95.2\text{mm}$$

The total mid-span deflection in the bridge (prototype) is 95.2mm due to a point load depicting the wheel load of 122,272N which is equivalent to 12.46tons which when the

scale factor is applied is equivalent to 24.93tons. The deck slab exhibited a pattern of punching shear, but its failure can be attributed to excessive deflections and maximum bending moments which could not redistribute over the supports as is the case in the actual deck slab. The 28MPa deck slab at failure exhibited the following failure pattern shown in Plate 4-8.



Plate 4-8 Failed Deck Slab – design strength of 30MPa.

4.3.3 13MPa Deck Slab (depicting the Design bridge condition):

The 13MPa deck slab was gradually loaded using the load cell with a point load concentrated at the middle of the deck slab. Cracks were observed to develop progressively from the centre of the deck slab outwards with fewer cracks observed longitudinally. The major effect that led to the failure of the 13MPa deck slab is the punching shear. The lower concrete strength implied that the effect of the increased localized loading led to the disintegration of the concrete at the point of load application. The punching shear consequently led to the formation of diagonal tension cracks in the loaded area, ultimately resulting in a conical failure at the top surface which was spread out on the bottom surface shown in Plate 4-9 and 4-10 below.



Plate 4-9 Progressive failure of the deck during the testing with punching shear observed

The first crack in the slab was observed at a load applied equivalent to 35kN (equivalent to 3.63tons) and was at a deflection of 39.00mm. In comparison to the 28MPa deck slab,

the first crack was observed at a loading of 107kN (10.93tons) with a deflection of 31.35mm. The structural steel did not suffer any failure but deformed in the same way as the concrete, which pattern was also observed in the bridge structure. This implies that structural steel provided sufficient tension resistance to resist the bending moment but couldn't resist or withstand the punching shear.



Plate 4-10 Total failure of the deck slab indicating that punching shear behaviour observed in the 13MPa deck slab was the main cause of failure for this model

Further loading was applied and the graph clearly indicates that with a smaller loading interval, much deeper cracks and deformations were obtained as compared to the behaviour prior to the first crack where a smaller deflection was obtained with a bigger loading interval. Total failure of the deck slab occurred when a load of 59 kN was applied (equivalent to 6.03 tons), and the total mid-span deflection of the 13 MPa deck slab was 91.20mm. The length scale factor used in the modelling was 2. It can be observed that there was a change in deflection from 20 to 32mm with a constant load of 29kN which implies lower strength of slab which couldn't carry the load any more leading to punching shear. However, hardening and stiffening due to the reinforcement bars resulted in resisting of the load hence more deflections with more loading. Plate 4-11 and Figure 4-12 below illustrate the above explanation.

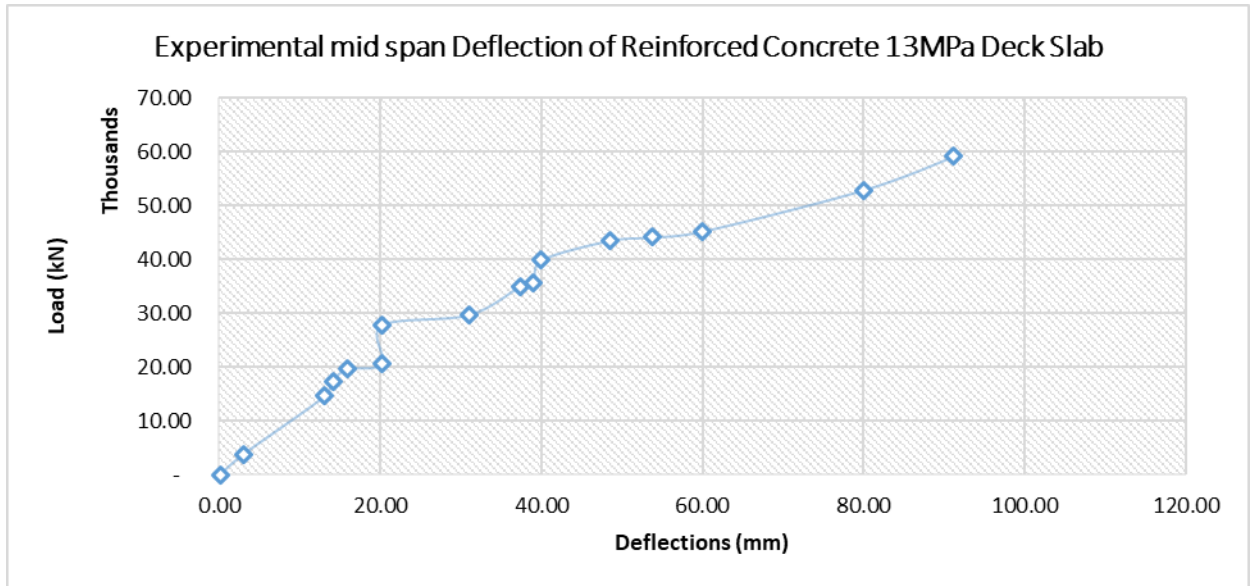


Figure 4-12 Graph for the Experimental mid-span deflection of the 13MPa Deck Slab

The 13MPa deck slab at failure exhibited the following failure pattern as shown below:



Plate 4-11 Failed Deck Slab – Indicates that the main cause of failure is punching shear regardless of the load but rather longitudinal cracking in the deck slab

4.4 NUMERICAL ANALYSIS OF THE HISTORIC BRIDGE

FE models of the tested part of the bridge deck slab and the entire bridge was made using the information obtained from section 1.1 Structural characterization of the failed historic bridge and from the non-destructive test results in section 4.1.5 Schmidt’s Rebound Hammer Test Results. Only the part of the slab in between adjacent longitudinal and transversal main beams was included in determining von-misses failure criterion. It was assumed that the boundary condition at the slab edges were fully restrained. The steel reinforcement of the deck slab panels was modelled as a reinforcement grid embedded in the shell elements. In each layer, a thickness corresponding to the reinforcement areas

shown in the drawings was provided in directions perpendicular to each other. A von Mises yield criterion was used for modelling the reinforcement material response. And initial yield strength equivalent to the average of the two determined during the test was used in the model.

The reinforcement was modelled as grid layers. The total reinforcement area for the reinforcement in a particular section was calculated and its equivalent thickness over a unit width was computed. The Von Mises plasticity model was used. The various input parameters for the steel properties was obtained from the test and used for the analysis and the results are included in appendix D. Detailed results of the numerical analysis are also attached in Appendix E.

4.4.1 Total Deformation of the entire bridge (Global Solution)

The solutions obtained from the analysis of the entire bridge indicated that the maximum deflection for the loading applied on the Bridge would be in either span of the Bridge but most especially on the first span from the Tororo – Mbale section of the Bridge which coincided with the actual failure of the Bridge as shown in Figures 4-13 and 4-14 below.

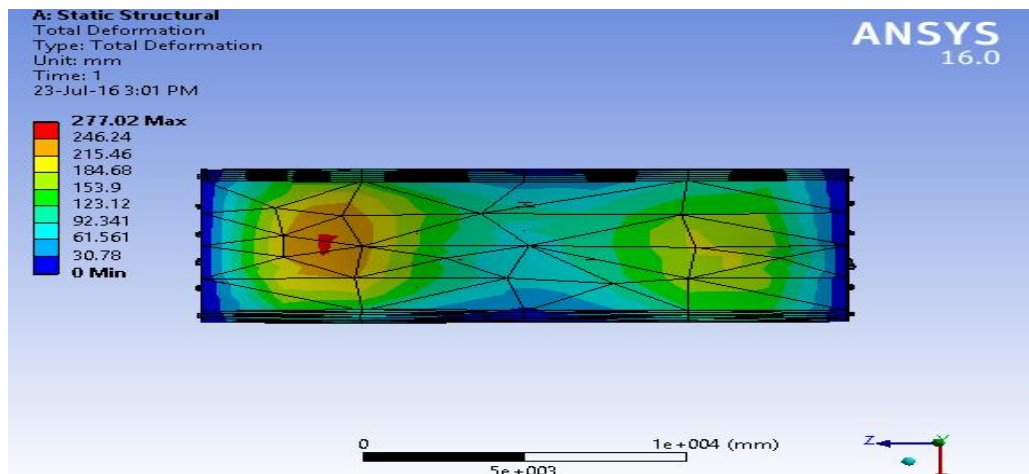


Figure 4-13 Total Deformation of the superstructure deck slab system (Top view)

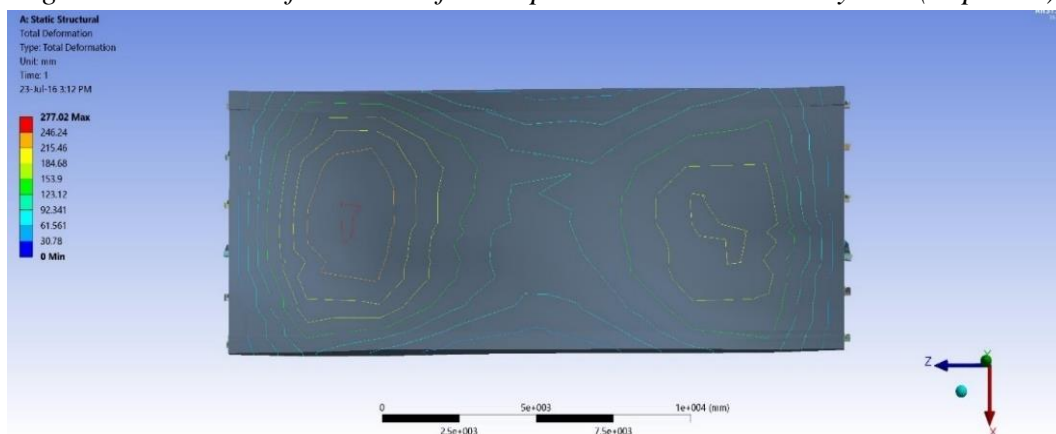


Figure 4-14 Total Deformation shown using contour lines of the superstructure deck slab system

4.4.2 Total Deformation of the Failed Bridge element (Particular Solution)

Unlike the global solution attained, a model of the specific section which failed (the part that developed a hole) was analyzed using ANSYS and its results closely followed or matched the experimental model. It indicated that if a point load was applied at the center of the slab by a wheel load (which as per the program is distributed along the entire slab), it would develop maximum stresses and deformations as indicated in the image below and as such would stretch out and be maximum at the edges outside the Steel I-beams as shown in Figure 4-12 below.

This indicates that this action was spread out on the entire bridge and the sections with the maximum loading result in the adjusting sections developing the highest deformations hence the failure. The half bridge solution as indicated in the Figure 4-20 shows that the maximum stresses and deformations will be towards the centre of the span for loading spread out within the entire bridge span.

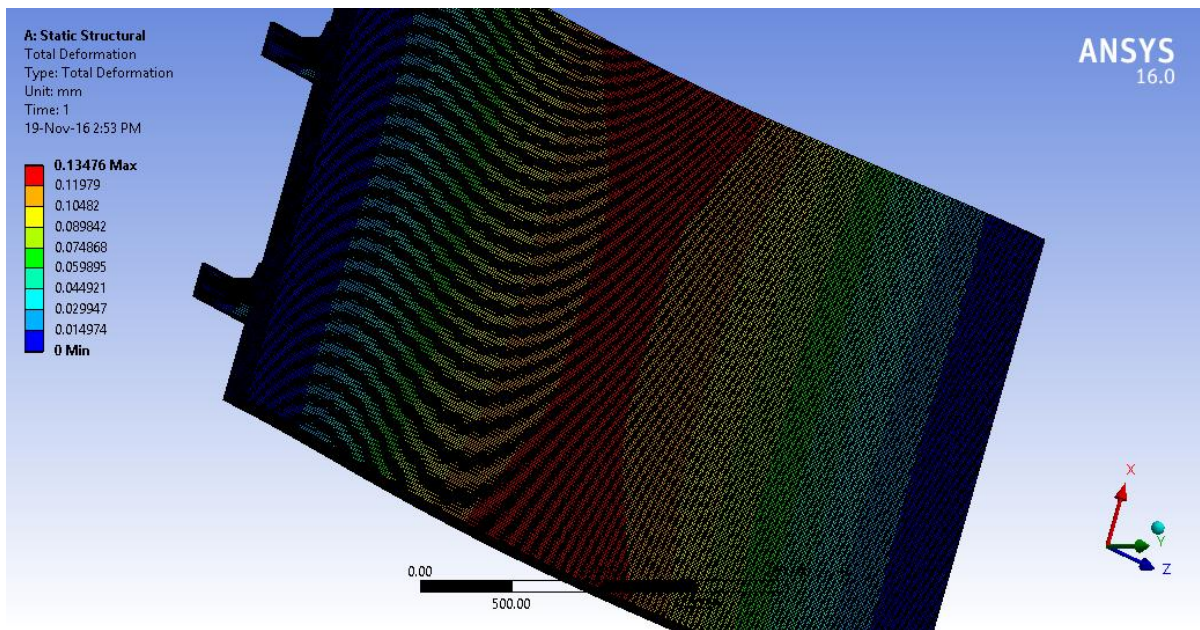


Plate 4-12 Total deformations of the failed bridge element

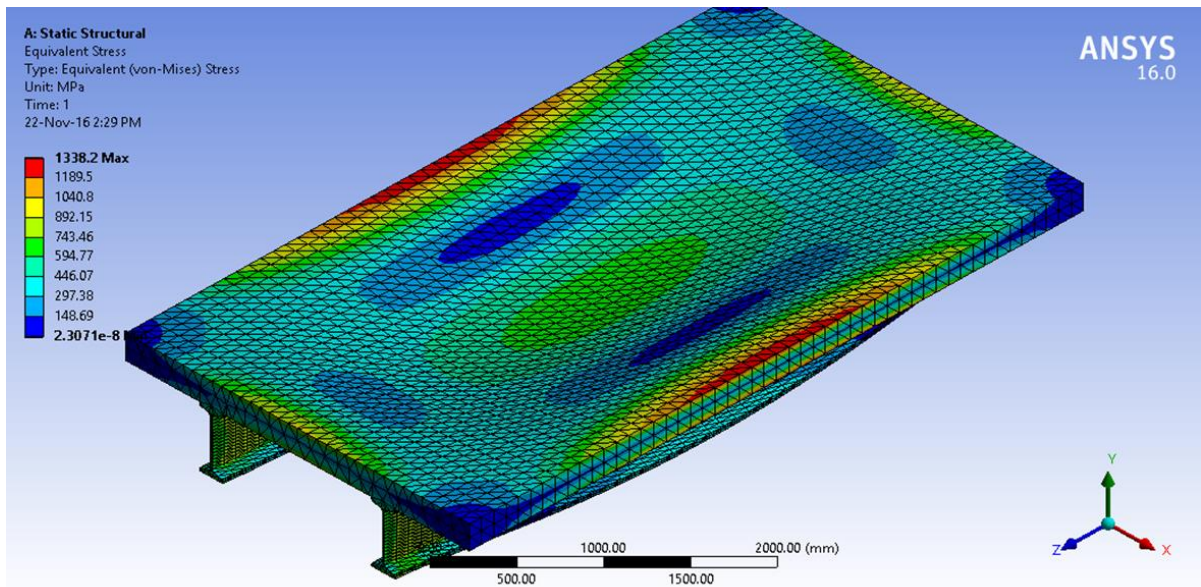


Figure 4-153 Von Misses Failure Criterion showing maximum stresses concentration

4.5 COMPARISON OF EXPERIMENTAL AND NUMERICAL ANALYSIS RESULTS

4.5.1 The Numerical analysis of the bridge failure model

The numerical model corresponds to the position where there is the observed behaviour of the bridge. The maximum deflection lies almost midway the width of the bridge at about 4 m from the edge (Tororo – Mbale direction) as is demonstrated in figure 4-16 below.



Figure 4-14 Comparison of the Numerical analysis results with the failure of the Manafwa Bridge

However, the deflection values obtained were very out of the range in comparison to the experimental results which is attributed to the failure to incorporate the reinforcements in the Reinforced Concrete Deck and little control over the functioning of the software. The results of the experimental model and the ANSYS analysis of the section also had significant similarities in the response to failure. The half bridge solution showed that the

maximum stresses and deformations will be towards the centre of the span for loading spread out within the entire bridge span. This to some extent corresponds to the actual failure in the bridge structure.

4.5.2 Structural Failure Mechanism using the Experimental Model

The total maximum deflection at the failure of the 13MPa deck slab model obtained is 91.20 mm at a maximum load of 59kN (6.03 tonnes) compared to the 30MPa deck slab obtained as 47.60 mm at a load of 122 kN (12.46kN). The failure in the deck slab depicting the design conditions of 28 MPa is by a combination of deformations, cracks and punching shear, with the main force at play being deformation. The punching shear consequently led to the formation of diagonal tension cracks in the loaded area, ultimately resulting in a conical failure at the top surface which was spread out on the bottom surface. The failure by punching in the experimental model closely relates to the actual failure of the bridge deck slab. The Plate 4-13 above shows a close semblance to the actual failure in the Bridge.



Plate 4-13 Failure in the Model compared to the actual failure in the bridge deck slab

On carrying out the visual inspections, it was observed that the concrete was just removed after failure for the inspection team to carry out investigations and to clearly demarcate the weak areas to avoid traffic or passengers from using it which may result into further damage. However, upon inquiring from the residents of the area, we were informed that the concrete did not completely collapse through the whole. This clearly shows that the model deck slab would have similarly failed in the same way if the loading was increased. These results are consistent with the numerical model and the experimental model.

Additionally, the failure in the bottom surface of the deck slab exhibited the same structural failure mechanism behaviour as the model tested in the laboratory. The cracks were very significant in the middle of the slab and spread out to the sides as demonstrated in Plate 4-14 below. However, there are much more cracks at the girder supports in the actual slab compared to the laboratory model which is most likely due to failure to depict the continuous effects of the deck slab.



Plate 4-14 Bottom surface Failure of the Experimental model 13MPa deck slab vs Actual Bridge structure

CHAPTER 5. CONCLUSION AND RECOMMENDATION

5.1 CONCLUSIONS

The Manafwa Bridge is comprised of a 20m long superstructure with a 200mm thick solid concrete slab cast on 6 steel I-section beams. The compressive strength of the deck slab had deteriorated and field results showed the low compressive strength of 13N/mm^2 in comparison to the design concrete strength class of 30N/mm^2 . Additionally, the tensile strength of the reinforcement bars had reduced from the design strength of 460N/mm^2 to 408.763 N/mm^2 for the R12 bars and 417.743 N/mm^2 for the R16 bars.

The study also demonstrated that the existing deck slab for the Manafwa Bridge was not adequate in punching shear for the in-situ concrete strength of 9.6N/mm^2 obtained but was adequate for the design strength of 30N/mm^2 and concluded that the Bridge could not have failed due to punching shear. The applied transverse sagging moments were all less than the slab moment capacities for the in-situ concrete strengths considered. This implies that there was a significant deterioration of the concrete which as a result could not withstand the applied moments hence the collapse. No hogging reinforcement was provided in the existing slab.

In the experimental modelling it was concluded that that main cause of failure of the deck slab was punching shear through the deteriorated concrete. At low load levels, flexural cracks developed at the bottom of the deck slab models directly under the loading area, within and around the loading perimeter. With load increase, radial cracks, that from literature review can be attributed to tangential moments, distributed out from the perimeter of the concentrated loading, breaking the slab into a fan-like fashion. When maximum load carrying capacity of the deck slab was reached as was the case for the Manafwa Bridge, shear cracking occurred from the tangential bending cracks and start building up a cone-like plug and ultimately into the hole that developed in the deck slab.

The numerical simulation of the failed deck slab section showed deflection patterns which were corresponding to the failure mode of the experimental model. The von misses failure criterion used for the stresses showed that the maximum stress concentration and deflection was in the centre of the deck slab which corresponded to the Manafwa Bridge failure positioning. Consequently, the numerical analysis using ANSYS adequately validated the results of the experimental modelling and the above-mentioned reasons for the failure of the Bridge.

5.2 RECOMMENDATIONS

5.2.1 Recommendations of the Research

The bridge should be repaired by providing a structural concrete topping slab of minimum class 30/25 structurally bonded to existing slab through use of shear connectors. Additionally, top hogging reinforcements should be provided. However, the Bridge was demolished. This is a very high cost to the country, and as such taking up this recommendation would have ensured the bridge serves for a much longer cost and priority given to new areas that require new bridges.

For other similarly constructed bridges that are still functional, the following should be done to enable them to be functional for an extended period:

- There is need to examine the provided shear connectors in the existing slab in order to reach a firm conclusion on whether the beams in these bridges are designed as composite sections or non-composite.
- The concrete strength of the existing slab should also be examined occasionally.
- A structural topping slab of 200mm thickness can be applied to the existing slab. The topping concrete should be of minimum Class 30/19 concrete structurally bonded to the existing slab. Top hogging reinforcement should be provided in the topping concrete with a concrete cover to the reinforcement of 40mm.

There is need to invest a lot more resources in acquiring of Numerical Analysis Software such as ANSYS, ABAQUS, DYNA and many others. In addition, it needs to source for personnel to train future students to ensure research is continuous.

5.2.2 Recommended Areas for Further Research

The destructive testing carried out in situ on the bridge was the coring test which had some limitations. The cores were used to only investigate the compressive strength of the concrete. In order to have a broader range of results and to understand in detail the failure mechanisms of the historic bridges, the extracted cores should be subjected to many other tests including chemical composition, durability tests of the concrete, fatigue analysis and they should be checked for the presence of deleterious matter. These parameters should then be incorporated into the numerical analysis and results reviewed for more detailed analysis of the failure mechanism as it has not been captured in this research.

REFERENCES

- ACI. (2014). *Building Code Requirements for Structural Concrete and Commentary*. Farmington Hills, Mich: ACI American Concrete Institute.
- Alenius, M., 2003. *Finite element modelling of composite bridge stability* (Doctoral dissertation, MSc Thesis Stockholm).
- Alexander, S., & Simmonds, S. (1986). *Shear-Moment Transfer in Slab Column Connections*. University of Alberta. Edmonton.
- Amir, S. (2014). *Compressive membrane action in prestressed concrete deck slabs*. PhD Thesis. Delft University of Technology, Delft.
- Aswa Bridge collapses. (2015, October 21). Retrieved December 11, 2015, from <http://www.newvision.co.ug/news/674734-aswa-bridge-collapses.html>
- Bagge, N. (2014). *Assessment of Concrete Bridges*. Lulea University of Technology, Lulea, Sweden.
- Bagge, N., & Elfren, L. (2016). Structural performance and failure loading of a 55 year-old prestressed concrete bridge. In *Maintenance, Monitoring, Safety, Risk and Resilience of Bridges and Bridge Networks*. (pp. 2225-2232). Lulea University of Technology: CRC Press, Taylor & Francis Group.
- Bagge, N., Nilimaa, J., Blanksvard, T., & Elfren, L. (2014). Instrumentation and Full-Scale Test of a Post-Tensioned Concrete Bridge. *Nordic Concrete Research*, 51, 63-83.
- Bagge, N., Shu, J., Plos, M., & Elfren, L. (2015). Punching Capacity of a Reinforced Concrete Bridge Deck Slab Loaded to Failure. In *Nordic Concrete Research: Residual Capacity of Deteriorated Concrete Structures* (pp. 57-60). Oslo, Norway.
- Biggs, R.M., Barton, F.W., Gomez, J.P., Massarelli, P.J. and McKeel Jr, W.T., 2000. *Finite element modelling and analysis of reinforced-concrete bridge decks* (No. FHWA/VTRC 01-R4,).
- CEN. (2004). *Eurocode 2: Design of concrete structures - part 1-1: General rules and rules for buildings*. Brussels, Belgium: CEN European Committee for Standardization.
- Chen, W. (Ed.), Duan, L. (Ed.). (1999). *Bridge Engineering Handbook*. Boca Raton: CRC Press.
- Fall, D., Shu, J., Rempling, R., Lundgren, K., & Zandi, K. (2014). Two-way Slabs: Experimental Investigation of Load Redistributions in Steel Fibre Reinforced Concrete. *Engineering Structures*, 80, 61-74.
- Fall, D., Shu, J., Rempling, R., Lundgren, K., & Zandi, K. (2014). Two-way Slabs: Experimental Investigation of Load Redistributions in Steel Fibre Reinforced Concrete. *Engineering Structures*, 80, 61-74.

- IS 13311 (Part-2) (1992) Methods of Non-Destructive Testing of Concrete: Part-2: Rebound Hammer
- IS 456 2000. Code of Practice for Plain and Reinforced Concrete,
- Kazungu, D. 2015. Manafwa Bridge develops cracks. Retrieved December 11, 2015, from <http://www.monitor.co.ug/News/National/Manafwa-Bridge-develops-cracks/-/688334/2617436/-/nwixowz/-/index.html>
- Kinnunen, S., & Nylander, H. (1960). *Punching of concrete slabs without shear reinforcement*. Transactions of the Royal Institute of Technology, No. 158, Stockholm, Sweden.
- Kudzys, a. (1999). Verification analysis of cast-in-situ reinforced concrete structures of framed multistory buildings. *Statyba*, 5(3), pp.193-199.
- Lantsoght, E., Veen, C., & Walraven, J. (2014). Shear in One-Way Slabs under Concentrated Load Close to Support. *ACI Structural Journal*, (110), 275-284.
- Li, H., 2012. Study on Durability Design and Critical Construction Technology for Concrete Bridges. Master Thesis. Zhengzhou, China: Zhengzhou Univerisy.
- Luttrell, L. (1987). *Design manual for composite decks, form decks and roof decks*. [Canton, Ohio]: The Institute.
- Miller, R., Aktan, A. F., & Shahrooz, B. M. (1994). Destructive Testing of Decommissioned Concrete Slab Bridge. *ASCE J Struct Div*, 120(7'), 2176-2198.
- Moe, J. (1961). *Shearing strength of reinforced concrete slabs and footings under concentrated loads*. Skokie, Ill.: Portland Cement Association, Research and Development Laboratories.
- Muttoni, A. & Fernandez Ruiz, M. (2008). Shear strength in one- and two-way slabs according to the Critical Shear Crack Theory. *Tailor Made Concrete Structures*, (1960), pp.559-563.
- Neville, A.M. (1981) *Properties of Concrete*. Longman Scientific & Technical, Pitman Publishing, London.
- Nilimaa, J. (2015). *Concrete bridges: Improved load capacity*. Ph.D. Thesis, Lulea University of Technology, Lulea.
- Nilimaa, J., Bagge, N., Blanksvard, T., & Taljsten, B. (2016). NSM CFRP Strengthening and Failure Loading of a Posttensioned Concrete Bridge. *Journal of Composites for Construction*, 20(3).
- Ogwang, J. (2012, July 2). UNRA prioritises repair, building of bridges. Retrieved December 11, 2015, from http://www.newvision.co.ug/newvision_cms/newsimages/file/edwin%201/8.pdf&usg=AFQjCNHP6MhKRG7FOltMPjLgk_EOCmM7
- Owilli, B., 2017. *Punching Shear Capacity of a Tested RC Bridge Deck Slab in Kiruna, Sweden*. Master's. Gothenburg, Sweden: Chalmers University Of Technology.

- Park, H., Chuang, E., Ulm, F.-J., 2003, Model-Based Optimization of Ultra High Performance Concrete Highway Bridge Girders, *Massachusetts Institute of Technology*, Cambridge, USA.
- Plos, M. (2002). Improved Bridge Assessment using Non-linear Finite Element Analyses. In *Bridge Maintenance, Safety and Management* (pp. 133-134).
- Plos, M., Shu, J., Zandi, K., & Lundgren, K. (2016): A Multi-level Structural Assessment Proposal for Reinforced Concrete Bridge Deck Slabs. *Structure and Infrastructure Engineering*, 13 (2), 223-241.
- Plos, M., Shu, J., Zandi, K., & Lundgren, K. (2016): A Multi-level Structural Assessment Proposal for Reinforced Concrete Bridge Deck Slabs. *Structure and Infrastructure Engineering*, 13 (2), 223-241.
- Pressley, J., Candy, C., Walton, B., & Sanjayan, J. (2004). Destructive Load Testing of Bridge No . 1049 - Analyses , Predictions and Testing. In *Fifth Austroads Bridge Conference, Hobart, Tasmania*. AUSTRROADS.
- Safi, M., 2009. Bridge Life Cycle Cost Optimization: Analysis, Evaluation & Implementation.
- Seshu, D. R., & Murthy, N. D. (2013). Non-Destructive Testing of Bridge Pier-A Case Study. *Procedia Engineering*, 54, 564-572.
- Shetty,MS (2010). Concrete Technology. S. Chand & Company, New Delhi.
- Shu, J., Bagge, N., Plos, M., Johansson, M., Yang, Y., & Zandi, K. (2016). Shear and Punching Capacity of a Field Failure Tested RC Bridge Deck Slab. *ASCE Journal of Structural Engineering*.
- Shu, J., Bagge, N., Plos, M., Johansson, M., Yang, Y., & Zandi, K. (2016). Shear and Punching Capacity of a Field Failure Tested RC Bridge Deck Slab. *ASCE Journal of Structural Engineering*.
- Shu, J., Belletti, B., Muttoni, A., Plos, M., & Scolari, M., (2016). Internal Force Distribution in RC Slabs Subjected to Punching Shear: Shell and Continuum Non-linear FE Analyses. *Engineering Structures*.
- Shu, J., Belletti, B., Muttoni, A., Plos, M., & Scolari, M., (2016). Internal Force Distribution in RC Slabs Subjected to Punching Shear: Shell and Continuum Non-linear FE Analyses. *Engineering Structures*.
- Shu, J., Fall, D., Plos, M., Zandi, K., & Lundgren, K. (2015). Development of Modelling Strategies for Two-way RC Slabs. *Engineering Structures*, 101, 439-449.
- Shu, J., Fall, D., Plos, M., Zandi, K., & Lundgren, K. (2015). Development of Modelling Strategies for Two-way RC Slabs. *Engineering Structures*, 101, 439-449.
- Shu, J., Plos, M., Johansson, M., Zandi, K., & Nilenius, F. (2016). Prediction of Punching Behaviour of RC Slabs Using Continuum Non-linear FE Analysis. *Engineering Structures*, 125, 15-25.

- Shu, J., Plos, M., Johansson, M., Zandi, K., & Nilenius, F. (2016). Prediction of Punching Behaviour of RC Slabs Using Continuum Non-linear FE Analysis. *Engineering Structures*, 125, 15-25.
- Spasojevic, A., 2006. Possibilities for Structural Improvements in the Design of Concrete Bridges. In *Proceedings of the 6th Int. PhD Symposium in Civil Engineering, Zurich 2006* (No. EPFL-CONF-111707, p. 8). Proceedings of the 6th Int. PhD Symposium in Civil Engineering, Zurich 2006.
- Talbot, A. (1913). Reinforced concrete wall footings. University of Illinois, Engineering Experiment Station. *Bull.*, 67, 114.
- Tassinari, L. (2011). *Punching Shear Tests on Reinforced Concrete Slabs with Non-symmetrical Reinforcement*. PhD Thesis, Ecole Polytechnique Federale de Lausanne, Lausanne.
- Taylor, R., Maher, D. R. H., & Hayes, B. (1966). Effect of the arrangement of reinforcement on the behaviour of reinforced concrete slabs. *Magazine of Concrete Research*, 18(55), 85-94.
- Tonias, D. and Zhao, J. (2018). *Bridge engineering: design, rehabilitation, and maintenance of modern highway bridges*. [online] Trid.trb.org. Available at: <https://trid.trb.org/view/1155243> [Accessed 28 May 2018].
- Troxell, G., Davis, H. And Kelly, J. (2018). *Composition And Properties Of Concrete*. [Online] Trid.Trb.Org. Available At: <https://Trid.Trb.Org/View/98960> [Accessed 28 May 2018].
- Tur, V. and Derechennik, S. (2018). Assessment of the Concrete Compressive Strength in Existing Structures Based on Core Test Results. *Solid State Phenomena*, 272, pp.238-243.
- Vaz Rodrigues, R., Fernandez Ruiz, M., & Muttoni, A. (2008). Shear strength of R/C bridge cantilever slabs. *Engineering Structures*, 30(11), 3024-3033.
- Veletzos, M.J., Panagiutou, M., Restrepo, J.I. and Sahs, S., 2008. Visual Inspection & Capacity Assessment of Earthquake Damaged Reinforced Concrete Bridge Elements (No. SSRP-06/19).
- Wang, Z., 2006. Life-cycle Analysis of Construction Project Based on the Durability of Concrete. Shanghai, China: Tongji University.
- Wilson, M., 2011. *Design and Control of Concrete Mixtures [Paperback]* 15th Ed. Amazon.com: Portland Cement Assn (2011). ISBN 10: 0893122726
- Wu, H., 2012. Environment Classification Based on Concrete Durability of Reinforced Concrete Structures. Ph.D. Thesis. Hangzhou, China: Zhejiang University Civil Engineering.
- Zandi Hanjari, K., Kettil, P., & Lundgren, K. (2013). Modeling the Structural Behavior of Frost- damaged Reinforced Concrete Structures. *Structure and Infrastructure Engineering*, 9(5), 416-431.

- Zhang, H., 2012. *Research on Improving Structural Durability of Highway Concrete*. Master Thesis. Jinan, China: Shandong University.
- Zheng, Y., Robinson, D., Taylor, S., & Cleland, D. (2009). Finite element investigation of the structural behaviour of deck slabs in composite bridges. *Engineering Structures*, 31(8), 1762-1776.

APPENDIX

APPENDIX A. STRUCTURAL CHARACTERISATION TEST RESULTS FROM THE REBOUND HAMMER

In-Situ Concrete Strength Test Results From The Rebound Hammer of the deck slab and parapet wall



PROJECT:	STRUCTURAL CHARACTERISATION AND PERFORMANCE EVALUATION OF THE FAILED MANAFWA HISTORIC BRIDGE IN UGANDA									
LOCATION:	Manafwa Bridge									
IN-SITU CONCRETE STRENGTH TEST RESULTS FROM THE SCHMIDT REBOUND HAMMER										
Testing Age:	>30days						Technician:			
	DECK SLAB						PARAPET WALL			
1	12.00	12.00	26.00	28.00	26.00	22.00	32.00	44.00	40.00	34.00
2	16.00	12.00	30.00	18.00	20.00	20.00	28.00	48.00	38.00	37.00
3	14.00	12.00	28.00	18.00	22.00	22.00	32.00	46.00	32.00	36.00
4	12.00	12.00	32.00	24.00	24.00	20.00	30.00	38.00	38.00	37.00
5	16.00	12.00	28.00	24.00	20.00	18.00	30.00	48.00	28.00	34.00
6	12.00	14.00	34.00	20.00	18.00	24.00	34.00	44.00	30.00	35.00
7	12.00	12.00	28.00	22.00	22.00	28.00	34.00	38.00	28.00	35.00
8	18.00	12.00	28.00	28.00	20.00	22.00	38.00	38.00	30.00	35.00
9	20.00	8.00	38.00	20.00	18.00	18.00	32.00	40.00	28.00	36.00
10	14.00	10.00	28.00	28.00	20.00	18.00	30.00	36.00	32.00	36.00
Mean	14.6	11.6	30.0	23.0	21.0	21.2	32.0	42.0	32.4	35.5
Std Dev	2.8	1.6	3.7	4.0	2.5	3.2	2.8	4.5	4.6	1.1
CV%	19.4	13.6	12.2	17.5	12.1	14.9	8.8	10.8	14.2	3.0
Compressive Strength (N/mm²) as read from chart	6.0	4.0	24.4	16.0	13.5	14.0	23.0	37.0	23.5	28.0
Average Compressive Strength (N/mm²)	13.0						27.9			

In-Situ Concrete Strength Test Results From The Rebound Hammer of the abutments, piers and footing

PROJECT:	STRUCTURAL CHARACTERISATION AND PERFORMANCE EVALUATION OF THE FAILED MANAFWA HISTORIC BRIDGE IN UGANDA								
LOCATION:	Manafwa Bridge								
IN-SITU CONCRETE STRENGTH TEST RESULTS FROM THE SCHMIDT REBOUND HAMMER									
Testing Age:	>30days								
	ABUTMENTS			PIERS					
1	42	20	38	28	36	26	44	26	26
2	44	24	44	40	34	22	55	24	18
3	38	26	40	22	30	28	24	26	60
4	40	28	48	36	30	24	26	30	28
5	38	22	38	32	44	26	28	30	40
6	30	28	32	34	32	28	36	26	30
7	36	24	44	36	28	30	28	18	28
8	32	22	36	28	32	26	28	26	38
9	34	20	36	30	30	26	26	24	34
10	32	22	40	32	34	22	36	24	36
Mean	36.6	23.6	39.6	31.8	33	25.8	33.1	25.4	33.8
Std Dev	4.6	3.0	4.7	5.1	4.5	2.6	9.9	3.4	11.3
CV%	12.6	12.5	11.9	16.1	13.8	10.0	29.8	13.4	33.3
Compressive Strength (N/mm²) from chart	34.0	18.0	39.0	26.4	28.5	19.5	29.2	19.0	30.0
Average Compressive Strength (N/mm²)	30			25			26		

APPENDIX B. DESTRUCTIVE TEST RESULTS FROM THE CORES TAKEN

Crushing Strength OF Cylindrical Cores obtained from the Bridge

 <div style="text-align: center;"> PAN AFRICAN UNIVERSITY INSTITUTE FOR BASIC SCIENCES, TECHNOLOGY AND INNOVATION </div> 														
STRUCTURAL CHARACTERISATION AND PERFORMANCE EVALUATION OF THE FAILED MANAFWA HISTORIC BRIDGE IN UGANDA														
Road Name: Tororo - Mbale Road														
Location :		Manafwa Bridge												
CRUSHING STRENGTH OF Cylindrical Cores obtained from the Bridge														
				Diameter =		145		Area =		0.01708929 m ²				
Sample No.	Location of the Core	Structural element	Side	Length	L/D	Remarks	Dimmension	Weight	Density	Crushing Load	Ultimate Compressive Strength	Correction Factor	Corrected compressive strength	Mean Strength
							LXBXH (mm)	(kg)	(kg/m ³)	(KN)	(N/mm ²)			
A	Km 0+0014 offset 4.40m from road edge	Deck Slab	RHS	160	1.1	Cores had a top layer of oil and Asphalt which was removed to expose the concrete	Ø145*160	6.310	2308	140	8.2	0.89	7.3	9.6
B	Km 0+0083 offset 5.20m		Centre	100	0.7		Ø145*100	4.050	2370	160	9.4	0.80	7.4	
C	Km 0+0064 offset 6.3 m		LHS	175	1.2		Ø145*175	6.820	2320	190	11.1	0.92	10.2	

APPENDIX C. STRUCTURAL STEEL LABORATORY TEST RESULTS

Tensile Strength Test For The R12 Rebar Obtained From The Deck Slab

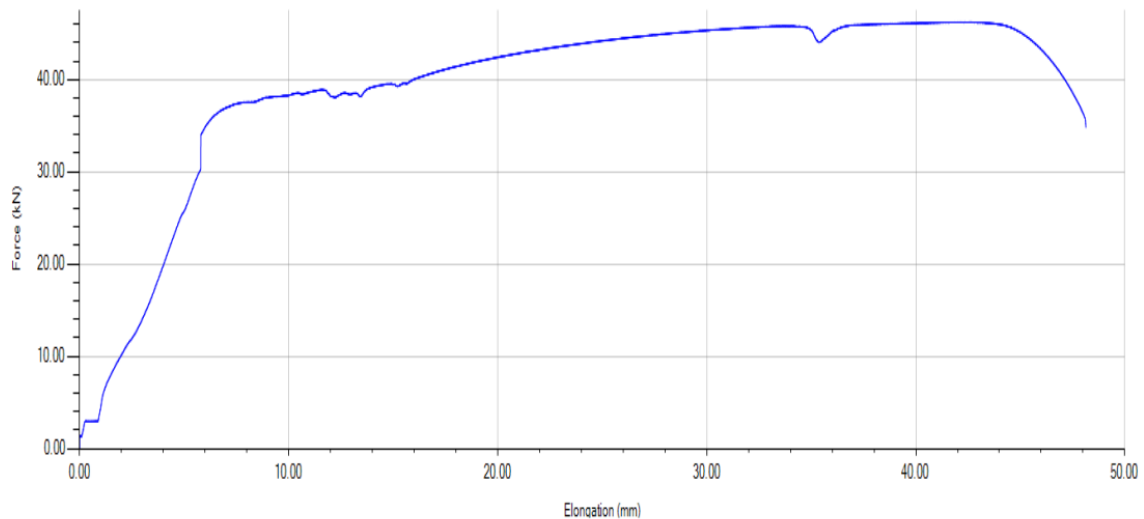
TENSILE TEST

Iga Ivan

Ref 1 : ROUND BAR 12mm
Ref 2 : GL-62.36mm
Ref 3 :

Machine No. : 0300-02032
Test Name : Tensile tests
Test Type : Tensile
Test Date : 19/04/2016 11:53
Test Speed : 8.000 mm/min
Pretension : 0.001 kN
Sample Length : 62.360 mm

Sample Code	Time of Test	Force @ Peak (N)	Stress @ Peak (N/mm ²)	Force @ Upper Yield (N)	Stress @ Upper Yield (N/mm ²)	Force @ 10.000 % Proof (N)	Stress @ 10.000 % Proof (N/mm ²)	Elongation after Fracture (mm)	Diameter (mm)
	19/04 11:58	46230.000	408.763	37119.999	328.213	38200.001	337.762	19.240	12.000



Tensile strength test for the R16 rebar obtained from the deck slab

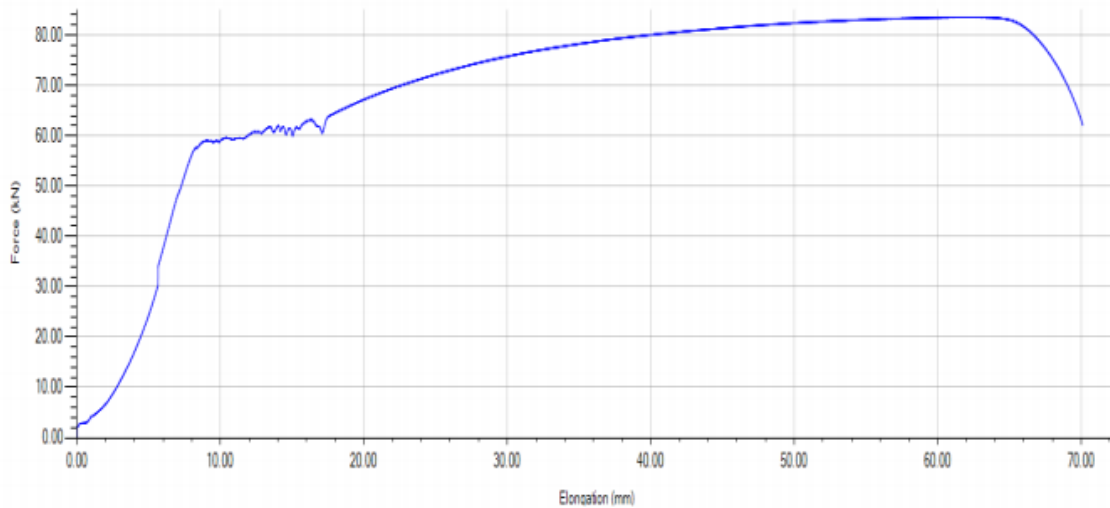
TENSILE TEST

subtitle test 1

Ref 1 : ROUND BAR 16mm
 Ref 2 : GL-78.2mm
 Ref 3 :

Machine No. : 0300-02032
 Test Name : Tensile tests
 Test Type : Tensile
 Test Date : 19/04/2016 12:12
 Test Speed : 8.000 mm/min
 Pretension : 0.001 kN
 Sample Length : 78.620 mm

Sample Code	Time of Test	Force @ Peak (N)	Stress @ Peak (N/mm ²)	Force @ Upper Yield (N)	Stress @ Upper Yield (N/mm ²)	Force @ 10.000 % Proof (N)	Stress @ 10.000 % Proof (N/mm ²)	Elongation after Fracture (mm)	Diameter (mm)
	19/04 12:13	83589.996	415.743	58880.001	292.845	71179.181	354.016	26.080	16.000



APPENDIX D.

APPENDIX E. NUMERICAL ANALYSIS DATA

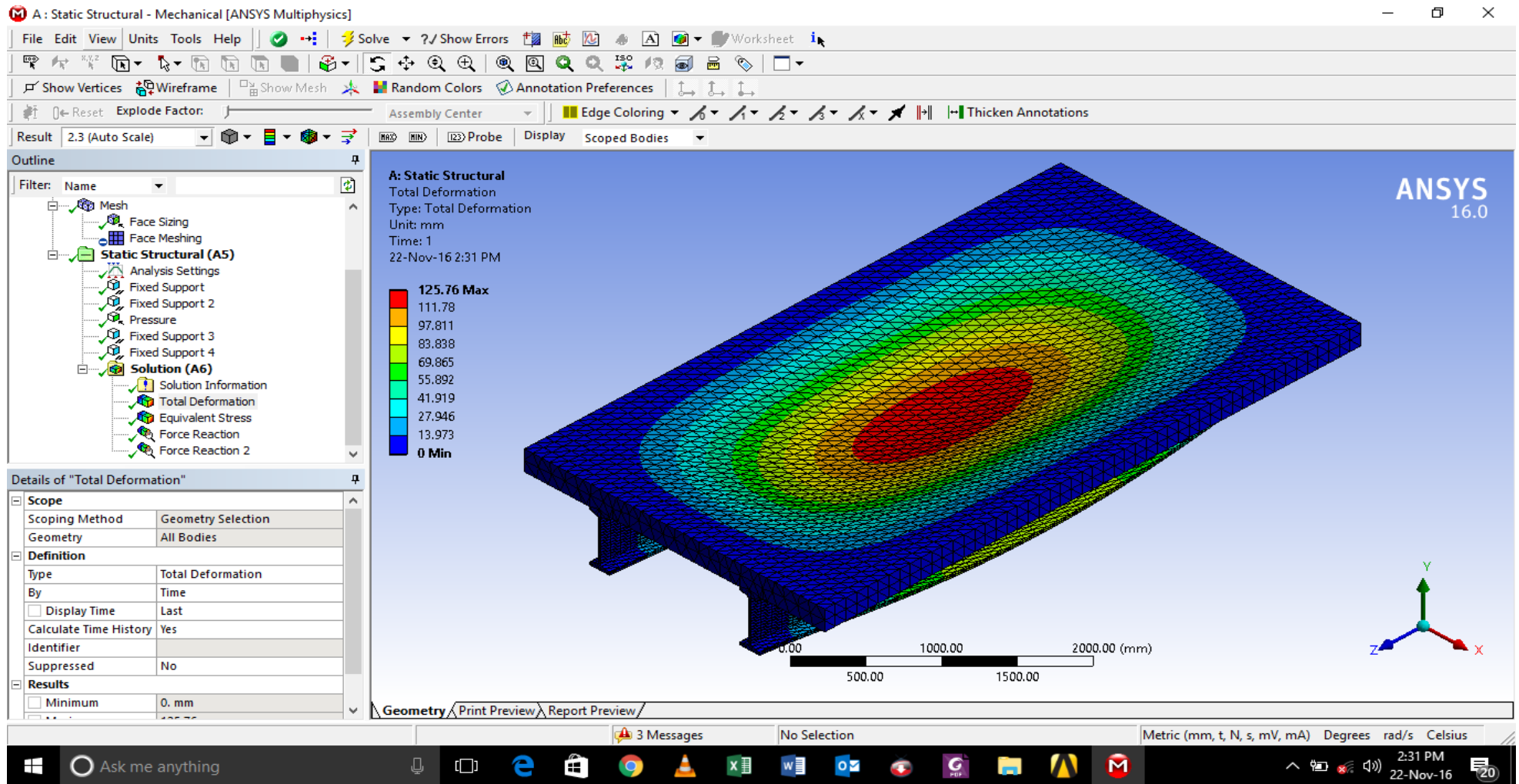
Model (A4) > Analysis

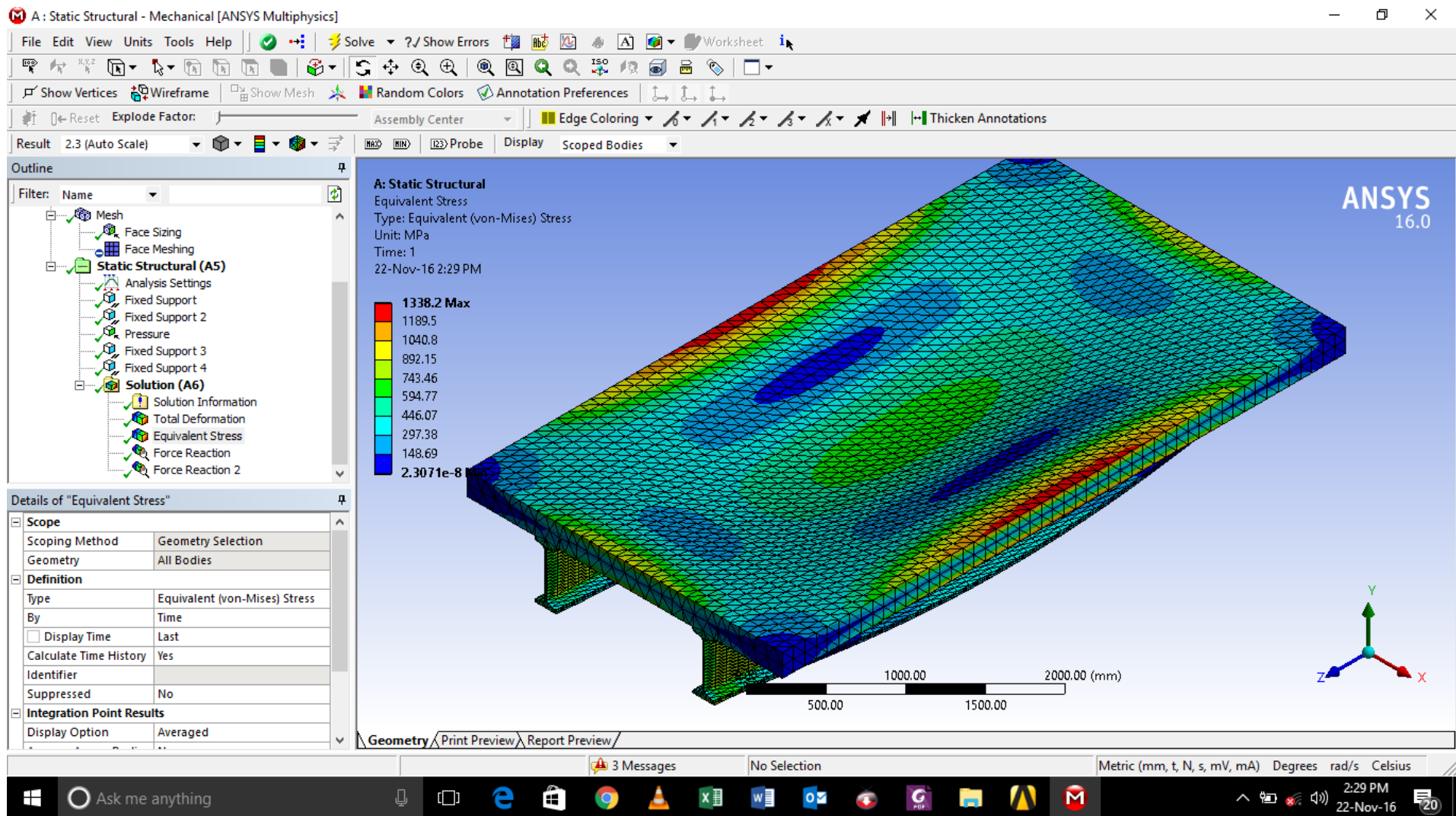
Object Name	<i>Static Structural (A5)</i>
State	Solved
Definition	
Physics Type	Structural
Analysis Type	Static Structural
Solver Target	Mechanical APDL
Options	
Environment Temperature	22.0°C
Generate Input Only	No

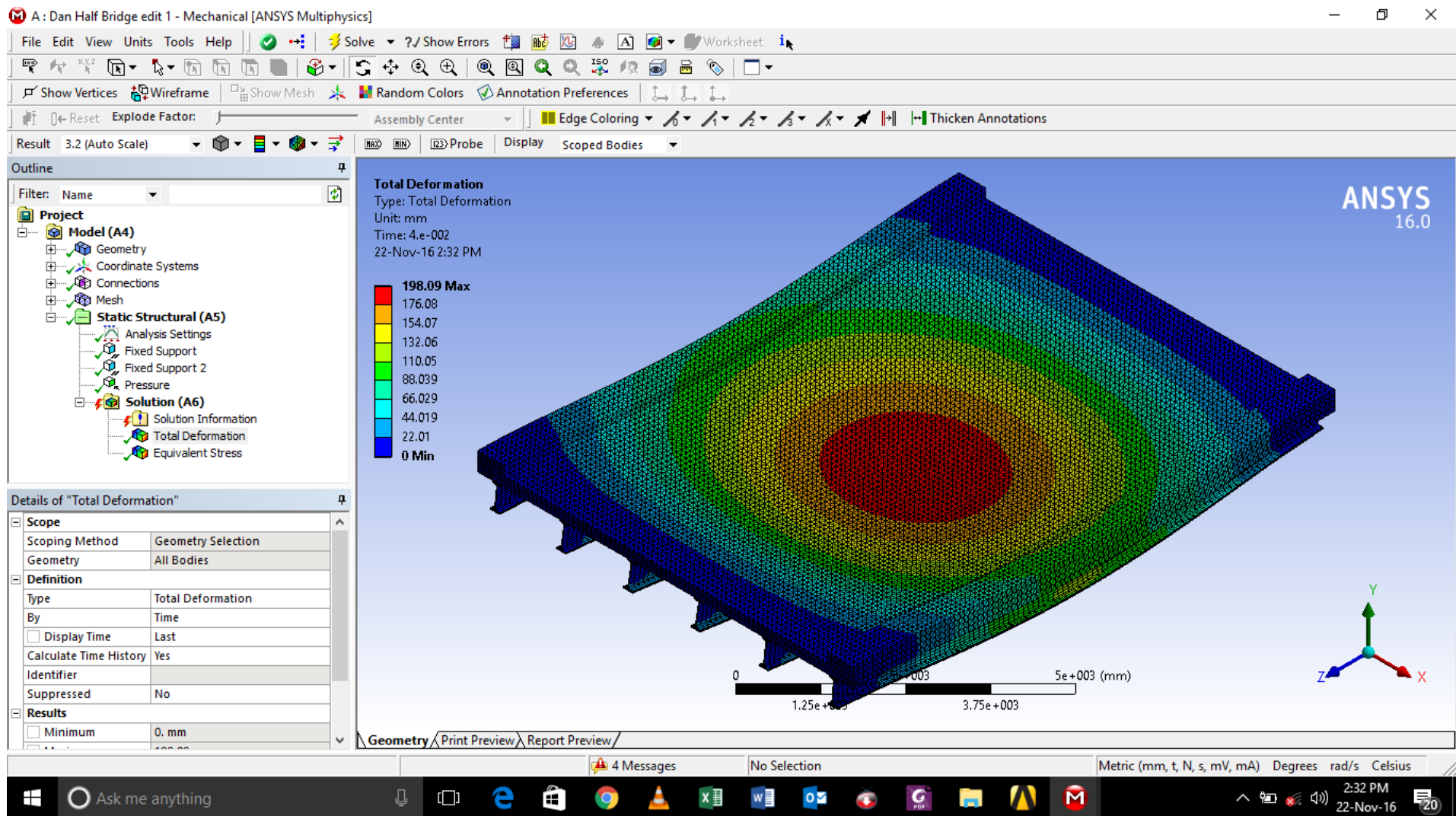
Model (A4) > Geometry

Object Name	Geometry
State	Fully Defined
Definition	
Type	Iges
Length Unit	Meters
Element Control	Program Controlled
Display Style	Body Color
Bounding Box	
Length X	7800. mm
Length Y	898. mm
Length Z	20000 mm
Volume	3.7856e+010 mm ³
Mass	1.0081e+005 kg
Scale Factor Value	1.

APPENDIX F. NUMERICAL ANALYSIS RESULTS DURING EVALUATION







APPENDIX G. EXPERIMENTAL TEST RESULTS

Results obtained from the practical testing of the 13MPa RC Slab

Load cell reading (mm)	LVDT reading (mm)	Actual Load (kg)	Experimental midspan deflection (mm)	Actual Load (kN)	Remarks
8	4	128	0.20	1256	
22	41	352	2.05	3453	
23	61	368	3.05	3610	
23	68	368	3.40	3610	
28	69	448	3.45	4395	
49	99	784	4.95	7691	
72	117	1152	5.85	11301	
100	628	1600	31.40	15696	
107	642	1712	32.10	16795	
129	669	2064	33.45	20248	
140	658	2240	32.90	21974	
170	680	2720	34.00	26683	
200	696	3200	34.80	31392	
225	706	3600	35.30	35316	
249	714	3984	35.70	39083	
272	718	4352	35.90	42693	
307	729	4912	36.45	48187	
370	747	5920	37.35	58075	
424	762	6784	38.10	66551	
476	777	7616	38.85	74713	
528	785	8448	39.25	82875	
568	798	9088	39.90	89153	
606	807	9696	40.35	95118	
653	819	10448	40.95	102495	
681	820	10896	41.00	106890	
724	833	11584	41.65	113639	
766	850	12256	42.50	120231	
804	859	12864	42.95	126196	
824	866	13184	43.30	129335	First Crack
902	879	14432	43.95	141578	
942	888	15072	44.40	147856	
969	901	15504	45.05	152094	
1041	917	16656	45.85	163395	

1085	922	17360	46.10	170302	
1113	931	17808	46.55	174696	
1172	945	18752	47.25	183957	
1252	956	20032	47.80	196514	
1284	961	20544	48.05	201537	Failure

Results obtained from the practical testing of the 30MPa RC Slab

Load cell reading (mm)	LVDT reading (mm)	Actual Load (kg)	Experimental midspan deflection (mm)	Actual Load (kN)	Remarks
28	65	448	3.25	4395	
29	70	464	3.50	4552	
31	79	496	3.95	4866	
47	90	752	4.50	7377	
51	95	816	4.75	8005	
70	106	1120	5.30	10987	
79	112	1264	5.60	12400	
92	119	1472	5.95	14440	
109	130	1744	6.50	17109	
108	130	1728	6.50	16952	
161	151	2576	7.55	25271	
163	155	2608	7.75	25584	
193	161	3088	8.05	30293	
209	173	3344	8.65	32805	
226	184	3616	9.20	35473	
237	187	3792	9.35	37200	
262	179	4192	8.95	41124	
259	180	4144	9.00	40653	
294	208	4704	10.40	46146	
298	210	4768	10.50	46774	
329	227	5264	11.35	51640	
368	235	5888	11.75	57761	
411	258	6576	12.90	64511	
441	267	7056	13.35	69219	
484	266	7744	13.30	75969	
514	288	8224	14.40	80677	
553	309	8848	15.45	86799	
611	326	9776	16.30	95903	
652	337	10432	16.85	102338	First

					Crack
697	350	11152	17.50	109401	
738	367	11808	18.35	115836	
778	378	12448	18.90	122115	
827	392	13232	19.60	129806	
881	412	14096	20.60	138282	
927	422	14832	21.10	145502	
978	440	15648	22.00	153507	
1061	460	16976	23.00	166535	
1104	476	17664	23.80	173284	
1149	484	18384	24.20	180347	
1192	499	19072	24.95	187096	
1300	521	20800	26.05	204048	
1404	529	22464	26.45	220372	
2240	742	35840	37.10	351590	

1 η = 16 kg

500 η = 25

mm

APPENDIX H. STANDARD VEHICLE CLASSIFICATION CHART









Table 1 Standard vehicle classification chart

<i>Category</i>	<i>Type of vehicle</i>	<i>Description</i>
1 Light vehicles		
1a	Motorcycles, etc	Motorcycles (with or without side-cars, e.g. motor tricycles).
1b	Passenger cars	Includes passenger cars seating not more than nine persons, estate cars, hire cars and taxis.
1c	Small buses	Includes minibuses, jeepneys, matatus, etc. Usually less than 40 seats.
1d	Light goods	
2 Medium and heavy vehicles		
2a	Large buses	All regular large passenger vehicles and coaches. This category does not include minibuses, jeepneys, matatus, etc. Usually more than 40 seats.
2b	Medium goods	2-axled vehicles with twin tyres on rear axle, more than 1.5 tonnes unladen weight but not exceeding 8.5 tonnes gross vehicle weight.
2c	Heavy goods (3 axles)	Larger trucks with three axles.
2d	Heavy goods (4 or more axles)	Vehicles with four or more axles (trailers being included as part of the vehicle) or exceeding 8.5 tonnes gross vehicle weight. Heavy vehicles may also be defined as those with an unladen weight of 3.0 tonnes or more.
3 Others		
		Includes miscellaneous vehicles such as tractors, road rollers, etc.. Many different types of vehicle could be recorded here. The type will depend upon factors including the purpose of the survey, the transport modes widely used in a particular country and the survey location. For example: i) for roads with high flows of multi-axled commercial vehicles, trucks with five or more axles and trucks with trailers could all be identified separately; ii) rickshaws, bicycles or tricycles could be recorded since large flows can be important when designing road width and geometry.

APPENDIX I. FORM FOR MANUAL CLASSIFIED TRAFFIC COUNTS

TRAFFIC COUNT FORM
 for Manual Classified Count

Location of survey: _____ Time of count: From _____ to _____
 Day of week: Mon / Tues / Wed / Thurs / Fri / Sat / Sun Date of count (DD/MM/YYYY): _____
 Enumerator name: _____ Weather: mainly: heavy rain / light rain / dry

	TRAFFIC DIRECTION: To _____												
	HOURS ENDING												
MOTORBIKE, + motor tricycle, etc													Total:
													
CAR, + taxis, etc													Total:
													
SMALL BUS (+ jeepney, etc)													Total:
													
SMALL TRUCK (2 axles, single rear tyres)													Total:
													
SUBTOTAL													Total:
Commercial vehicles (for pavement design purposes):													
LARGE BUS													Total:
													
MEDIUM TRUCK (2 AXLES, with twin rear tyres)													Total:
													
HEAVY TRUCK (3 AXLES)													Total:
													
HEAVY TRUCK (4 or more AXLES)													Total:
													
OTHER (to be defined)													Total:
SUBTOTAL													Total:

Sheet no. _____ of _____ Total:

APPENDIX J. TRAFFIC DATA COLLECTED AND ANALYSED

Vehicle Class	Axles Load / kg	EALF (Axles/8160)	Average per day	ESAL
Pedestrians				
Bicycles				
Motorcycles				
Saloon cars and taxis	1000	0.12254902	332	40.68627
Light Goods Vans: (Pickups, 4WD)	2000	0.245098039		0
Small Bus: Minibuses and Matatus	3000	0.367647059	31	11.39706
Medium Bus: Coasters	4500	0.551470588		0
Light Single Unit Trucks: Dynas and tractors	4000	0.490196078	96	47.05882
Medium-Large Single Unit Trucks: Lorries, fusos	7500	0.919117647	83	76.28676
Buses	10000	1.225490196	8	9.803922
Medium truck (2 axles with twin rear tyres)	18000	2.205882353	83	183.0882
Heavy truck (3 axles)	26000	3.18627451	27	86.02941
Heavy truck (4 axles)	38000	4.656862745	116	540.1961
				0
				0
TOTAL				994.547

APPENDIX K. EQUIPMENT LIST FOR TRAFFIC COUNT AND/OR AXLE LOAD SURVEY

Traffic count

- Shelter (for day and night, if required): including tent, blankets, large umbrella and chairs.
- Night-time lighting (if required). This is required to illuminate both the road (to aid identification of vehicle type) and the camp so that observers can see the forms.
- Generator for lighting (if necessary), plus fuel.
- Food and water. A large water container is essential. Cooking facilities may also be needed.
- Access to toilet facilities.
- Survey sheets (enough copies for the whole duration, plus spares).
- Clipboards and pens, pencils.
- Hand-counters (if required, for high traffic flows).
- Alarm clock (useful to mark the end of each hour and denote shift changes).

Axle load survey

- Axle load survey forms.
- Pens and stationery plus clipboards, folding table.
- Reflective safety vests.
- Road signs (for both directions if required) – e.g. 2x: ‘men at work’, ‘slow down’, ‘60 km/h’, ‘weighbridge ahead’, ‘30 km/h’, ‘prepare to stop’ and ‘stop’.
- Traffic cones.
- Red stop flags.
- Lights and cables (to light the weighing area, the data recording table and, if possible, the vehicle stopping area).
- Generator plus fuel.
- Torches (including spare batteries).
- Spade.

APPENDIX L. CONCRETE MIX DESIGN – SAMPLE FORM USED AND MATERIAL RESULTS

Mix Design for Concrete Grade = M 30

C1. Design stipulation:

- i Characteristic Compressive strength = N/mm²
- ii Maximum size of aggregate = mm
- iii Degree of workability =
- iv Degree of quality = Good
- v Type of Exposure = Mild

C2. Test data for materials

- (i) Cement used = PPC
- (ii) Specific gravity of Cement =
- (iii) Specific gravity
 - Fine Aggregate =
 - Coarse Aggregate =
- (iv) Water absorption
 - Fine Aggregate = %
 - Coarse Aggregate = %
- (v) Free Surface Moisture
 - Fine Aggregate = %
 - Coarse Aggregate = Nil %
- (vi) Fine Aggregate confirming the table 4, IS 383- Zone = Zone

C3. Target mean strength = N/mm²

C4. Selection of Water Cement ratio

Water Cement ratio = (From fig. 1, Is 10262)

C7. Determination of Fine & Coarse aggregate

Air entrapped in concrete = % (From Table 3, IS 10262)

Actual quantity of concrete "V" = 0.98 Cum

Materials required for concrete

Grade M 30

Concrete quantity = Cum

Sl. No	Material name	Quantity	Unit
1	Cement	126.82	kg
2	Fine Aggregate	52.37	kg
3	Coarse Aggregate 20mm	212.91	kg
4	Coarse Aggregate 10mm	141.94	kg
5	Water	16.50	ltr
6	Slump	75 - 100	mm
7	W/C ratio	0.44	

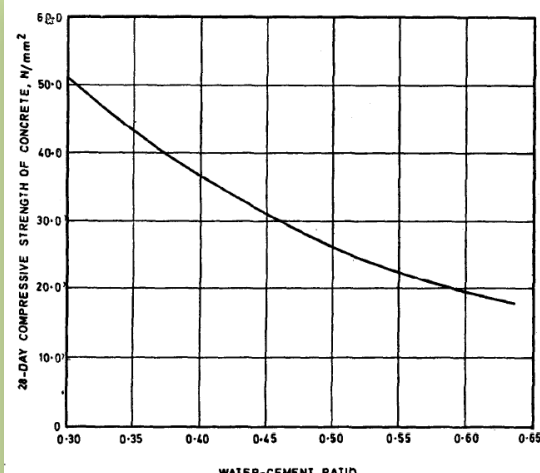


FIG. 1 GENERALISED RELATION BETWEEN FREE WATER-CEMENT RATIO AND COMPRESSIVE STRENGTH OF CONCRETE

Sieve analysis results for the sand

<i>Sieve Sizes (mm)</i>	<i>Wt. Retained</i>	<i>Wt. Retained%</i>	<i>Wt. cumm.</i>	<i>% cumm. Rt.</i>
10.00	1	0.1	0.1	0.01
5.00	24	2.4	2.5	0.25
2.36	45	4.5	7.0	0.70
1.70	54	5.4	12.4	1.24
1.20	145	14.5	26.9	2.69
0.60	278	27.8	54.7	5.47
0.30	314	31.4	86.1	8.61
0.15	118	11.8	97.9	9.79
<i>Pan</i>	21	2.1	-	
<i>Sum</i>			2.88	

APPENDIX M. BRIDGE INSPECTION REPORT – FILLED CONDITION
ASSESSMENT SURVEY FORM